Droplet Lasers

McGloin, David

Published in:
Reports on Progress in Physics

DOI:
10.1088/1361-6633/aa6172

Publication date:
2017

Document Version
Peer reviewed version

Droplet Lasers and Resonators

D.McGloin

SUPA, School of Science and Engineering, University of Dundee, Dundee DD1 4HN UK

E-mail: d.mcgloin@dundee.ac.uk

July 2015

Abstract. It is perhaps surprising that something as fragile as a microscopic droplet could possibly form a laser. In this article we will review some of the underpinning physics as to how this might be possible, and then examine the state of the art in the field. The technology to create and manipulate droplets will be examined, as will the different classes of droplet lasers. We discuss the rapidly developing fields of droplet biolasers, liquid crystal laser droplets and explore how droplet lasers could give rise to new bio and chemical sensing and analysis. The challenges that droplet lasers face in becoming robust devices, either as sensors or as photonic components in lab on a chip devices is assessed.

Submitted to: *Rep. Prog. Phys.*

1. Introduction

The first laser demonstration in 1960 by Theodore Maiman [1] probably fixes in the mind the classic idea of a laser resonator, and for anyone learning about the subject at high school, the simple schematic of a laser gain material sitting between two mirrors is one that will not need much amending throughout a future scientific career. However it is perhaps not so widely appreciated that one of the very earliest demonstrations of stimulated emission came in a much different experimental configuration, that of a spherical resonator [2]. The mirrors of the conventional resonator were replaced by another simple physical property we learn about at school, total internal reflection, enabling the sphere to act as a high quality resonator. If we fast forward to the present day, this early work has inspired much of the exciting development in high Q resonators and their applications in areas such as optomechanics [3].

The idea of a spherical laser resonator has application in a different direction. While much of the work on optomechanics centres around the idea of a stable solid resonator in spherical or disc form, there are other ways to make spheres than using what typically amounts to very small glass balls. Since the 1970s work has been carried out which makes use of liquid droplets acting as resonators, which is a natural extension of the physics behind a rainbow, but internalising all the light, rather than a double (or higher order) refraction process. The challenge is, of course, that droplets are inherently much less stable than solid particles, and are far more susceptible to environmental perturbations than their solid counterparts. They are also, in general, rather more difficult to control, to create and to handle.

Nevertheless, droplet resonators are indeed viable as lasers, and the sensitivity of droplets does give rise to some advantages, in terms of tunability and possibly detection sensitivity. Moreover for probing certain kinds of biological processes, the ability to encapsulate the system under study highlights an attractive benefit of liquid over solid. Limitations remain of course - droplet lasers, while offering microscopic sensing opportunities and the ability to probe basic light mater interactions, offer little opportunity for scaling, and the complexity of implementing environmental control systems may outweigh any advantages. The field remains buoyant despite these challenges, and new demonstrations look very promising in the field of biolasers moving away from simple droplet systems containing nothing but a laser dye.

In this report we will examine the field of droplet lasers, covering basic background theory, discuss related work in optomechanical and optofluidic sensing, offer a thorough review of the literature of the field and a commentary on the state of the art and future directions for the field.

1.1. Historical Development of Droplet Lasers

The first spherical resonator [2] to act as a laser was made from CaF_2:SM^{++}, cooled using liquid hydrogen and built at Bell Laboratories in 1961, figure 1. It was flash lamp pumped with a threshold of $20W/cm^2$. This work, as well as being one of the first works

in the laser era, drew on much older work, starting from the description of a "Whispering Gallery Mode" (WGM) first quantitatively examined by Lord Rayleigh in the early 20th century [4] [5]. Rayleigh considered a problem related to acoustic wave propagation in a spherical cavity, which is named after the 'Whispering Gallery' in St. Paul's Cathedral in London. In the Gallery, in the dome of the cathedral, sound can propagate around the internal surface such that a whisper at one side of the Gallery will propagate around to someone listening at some other point around the circumference. This basic piece of physics underpins the the ability to create droplet lasers.

Figure 1 about here.

Rayleigh's work would inspire others to examine how different types of waves would propagate in media other than free space, and another early piece of work relevant to spherical resonators was the work by Richtmeyer at Stanford in 1939 [6], where shaped dielectrics were considered and a spherical dielectric resonator was analysed on the way to more a complex dielectric ring, with a view to applications in electrical communication systems. The Richtmeyer analysis laid out that a Q value could be defined for such a resonator by:

$$Q = \omega \frac{\text{energy stored}}{\text{power radiated}}, \tag{1}$$

where ω is the angular frequency of the resonant field. Q values of the order of 10^6 were theoretically predicted indicating that such spheres could act as extremely high quality resonators. Richtmeyer also described the field in terms of the "resonant modes of oscillation" supported by the sphere. Exploitation of the ideas in the form of a laser would have to wait a further 22 years in the form of a sphere and a little later in the form of a ring, e.g. [7].

While droplet lasers were still someway off, one of the key challenges for their future development would be partially solved in the 1970s with the advent of optical manipulation techniques [8]. A droplet cannot easily rest on a surface without spreading, and so if one wishes to make a laser then the droplet must either pass through the excitation beam, or must be localised in some way. Arthur Askhin and colleagues over the course of a decade devised and refined techniques that could straightforwardly localise a particle in both liquid and in air [9]. These techniques worked using the radiation pressure of light to hold falling particles against gravity, making use of microscopic particles, rather than the much larger millimeter size particles previously. Thurn and Keifer also carried out similar work in the mid-1980s levitating solid spheres in air and taking Raman spectra from them [10].

Ashkin also made a further significant step towards a laser by showing that optical resonances could be observed in these micro-particles in the form of optically levitated droplets, both silcone oil [11] and subsequently in water [12]. The resonance peaks observed allowed the droplets to be sized very accurately, to around 1 part in 10^5 or 10^6 making use of Mie scattering theory.

The big breakthrough came from the main pioneering group of droplet lasers, Richard Chang's, working at Yale. In 1980 they reported the results of experiments to observe resonance in a *fluorescing* microsphere, laying the path for the first dye doped microparticle lasers. The polystyrene spheres used were $9.92\mu m$ in diameter, dispersed in water and were doped with an unspecified dye and pumped by a $457.9nm$ continuous wave Argon-ion laser. The excitation beam caused fluorescence to occur, which was then trapped within the cavity formed by the droplet, and resonance peaks associated with the cavity excited modes were then observed.

It was Chang's group who then took this one stage further producing, in 1984, the very first microdroplet laser, in a continuous flow of dye doped droplets [13]. Before discussing this work in more detail, we turn our attention to some of the background theory for whispering gallery mode resonators.

1.2. Whispering Gallery Mode Resonator Physics

We note that there a number of reviews looking at whispering gallery mode resonators, also called morphological dependent resonances (MDRs) mainly focusing on more general cavity types than droplets, however much of the basic theory is similar. Throughout this work, the terms WGM and MDR can be considered interchangeable, and appear in different contexts depending on how the original works involved made use of the terms; we will refer to WGMs. More detail can be found in [3, 14, 15, 16, 17] (among others) but we highlight the key concepts below.

In order to confine light within a droplet, the refractive index of the droplet must be higher than the surrounding medium to enable total internal reflection. This results in light that hits the droplet at greater than the critical angle, given by $\theta_c = sin^{-1}(n_s(\omega)/n_l(\omega))$, where n_s is the refractive index of the surrounding medium, n_l is the refractive index of the droplet liquid and ω is the frequency of the light. A simple cartoon of the optical confinement and the droplet mode structure can be seen in figure 13 (c) and (d).

Light trapped in such a spherical droplet can circulate a whole number of wavelengths must fit around the cavity:

$$2\pi r n_l = m\lambda \tag{2}$$

where λ is the wavelength of the light, and r is the droplet radius and m is the angular mode number, denoting the number of modes around the circumference of the droplet boundary. This is often expressed in terms of a size parameter, x, where $x = 2\pi r/\lambda$, noting that λ/n_l is the wavelength in the droplet medium.

The positions of the cavity resonances, taking account of the fact that the cavities can support both TE and TM modes, can be found using asymptotic or Lorenz-Mie calculations [18, 19] to be:

$$\lambda^{-1} = \frac{1}{2\pi r n_l}\left[m + \frac{1}{2} + 2^{-1/3}\alpha(p)\left(m + \frac{1}{2}\right)^{1/3} - \frac{\kappa}{(n_r^1 - 1)^{1/2}}\right.$$

$$+ \frac{3}{10}2^{-2/3}\alpha^2(p)\left(m+\frac{1}{2}\right)^{-1/3} - 2^{-1/3}\left(n_r^2-\frac{2}{3}\kappa^2\right)\frac{\alpha(p)\left(m+\frac{1}{2}\right)^{-2/3}}{(n_r^2-1)^{3/2}}\Bigg] \quad (3)$$

n_r is the relative refractive index $= n_l/n_s$ and L is the cavity circumference. For TE modes $\kappa = n_r$ and for TM modes, $\kappa = 1/n_r$. $\alpha(p)$ denote the roots of the Airy function. p is the radial mode number, which accounts for the number of modes along the radius of the droplet. A third quantum number can be defined, the azimuthal mode number, l, accounting for the modes in the azimuthal direction. In the case of the perfectly spherical resonator the m modes corresponding to a given l are degenerate ($2l$+1 modes). In the case of a droplet, deformation can lift the degeneracy, leading to a frequency for each mode given by [20]:

$$\omega(m) = \omega_0\left(1-\frac{e}{6}\left[1-\frac{3m^2}{l(l+1)}\right]\right) \quad (4)$$

where ω_0 is the frequency of the degenerate WGM in the undeformed sphere. e is the sphere eccentricity.

As noted above each optical cavity has an associated Q factor, which can be written, often in preference to equation (1) in the form $Q = \omega\tau$ where τ is the cavity ring-down lifetime, and is a different way of expressing the energy storing ability of the cavity.

This Q factor can then be broken down into a serious of components, each of which introduce loss into the system. These can be expressed as:

$$Q^{-1} = Q_{scatt}^{-1} + Q_{rad}^{-1} + Q_{mat}^{-1} + Q_{cont}^{-1} \quad (5)$$

where Q_{scatt} is the scattering loss factor due to surface inhomogeneity, Q_{rad} is the radiative loss factor and Q_{mat} is the material loss factor. The final loss factor is due to external contaminants during fabrication, Q_{cont}, and is specific to solid particles rather than liquid droplets, and so can be ignored in these applications.

The different Q factors can be expressed as follows:

$$Q_{scatt} = \frac{\lambda^2 r}{\pi^2\sigma_{rms}^2 B} \quad (6)$$

where σ_{rms} is the rms length of the surface inhomogeneity, B is the length of the inhomogeneity (also called the correlation length). The form of Q_{scatt} indicates that not only are homogeneous spheres far better cavities, but that larger cavities perform better than smaller ones. The surface inhomogeneity length is driven by thermal fluctuations and is given by [21]:

$$\sigma_{rms} = \left[\frac{k_B T}{4\pi\gamma}\right]^{1/2} \quad (7)$$

with γ being the surface tension of the droplet, k_B the Bolztmann constant and T the temperature. For a droplet made of water and glycerol, Jonáš *et al* [22] estimate

that for a $130\mu m$ diameter droplet that $\sigma_{rms} \approx 0.07$nm and B is $\approx 6.3nm$, giving $Q_{scatt} \approx 1.7 \times 10^{11}$. In the case of a droplet sitting on a hydrophobic surface [22], these fluctuations, for example, limit the effective measured Q factor to $\sim 10^6$.

The material loss factor is:

$$Q_{mat} = \frac{2\pi n_l}{\alpha\lambda} \tag{8}$$

The term α is the linear absorption coefficient and indicates that this is primarily a loss mechanism to do with absorption. For the droplet in [22] $Q_{mat} \approx 5 \times 10^7$.

Finally, the radiative loss accounts for losses due to the curvature of the cavity and again tend to be greater for smaller cavities with higher radii of curvature, Following [14] this has the form:

$$Q_{rad} \approx \frac{l}{n_l} \exp\left[2lg\left(\frac{1}{n_l}\right)\right] \times \exp\left[-2\sqrt{n_l^2 - 1}\frac{n_l x - l}{n_l}\right] \tag{9}$$

where $g(1/n_l) = -\sqrt{1-(1/n_l)^2} + \arg\cosh(n_l)$. x is the size parameter. Modes near the equator of the droplet will tend to have a higher overall Q value, and for perfect spheres, $Q_{rad} > 10^{11}$.

The measurement of the mode spectrum for a droplet is important as it enables the physical parameters of the droplet to be calculated. In particular the radius of the droplet can be found for the degenerate case by [23]:

$$r = \frac{\lambda^2}{2\pi n_s \Delta\lambda} \frac{tan^{-1}(n_r^2 - 1)^{1/2}}{(n_r^2 - 1)^{1/2}} \tag{10}$$

where $\Delta\lambda$ is the difference between two adjacent modes, λ_m and λ_{m+1}. Typically mode shifts will be observed as the droplet changes in size, but it has also been predicted recently that for droplets with a very low interfacial tension (making use, for example, of mixed oil phases for the droplet and surrounding media), that even a single photon may be able to induce radiation pressure based shifts [24]. This has, however, not been experimentally demonstrated yet, nor applied specifically to droplet lasers.

Interestingly in the majority of droplet laser work there is little consideration of the output power, other than to say there is a threshold and the output grows in the expected fashion for increasing pump power beyond this point. This is largely to do with the challenges in measuring the output definitively, and often for practical purposes the output seems to be almost too low to comfortably note. In the literature there is little detailed consideration of the laser characteristics, but there is some simple modeling considering the droplet as a ring dye laser [25, 26]. The output power from a typical dye laser droplet can be written as [25, 27]:

$$P_{out} \sim \frac{A(a,\lambda)}{\lambda^3} g_0(\lambda)\beta(a,\lambda) \tag{11}$$

where $A(a,\lambda)$ is lasing cross section of the WGMs, $\beta(a,\lambda)$ is the output efficiency and $g_0(\lambda)$ is the dye gain spectrum.

1.2.1. Whispering Gallery Mode Resonators as Sensors In this short section we make a slight digression from the main topic of this review, to consider what droplet lasers are not very good at, local sensing. The big challenge with droplets is the difficulty in monitoring perturbations to the droplet surface, and for most sensing applications this is typically where the particulates to be sensed will start. Even with droplets containing the particles of interest there are challenges with droplet size versus diffusion of the particle to a point within the cavity where the field is sufficient that any perturbation or change can be measured.

The broad field of whispering gallery mode sensors using solid cavities [15], [28] is mature and has a wide range of demonstrated sensing capabilities, as well as more fundamental applications in the study of optomechanics. This far and away outstrips the utility to date of droplet lasers, which are an unusual subset of active media within the typically passive cavity sensor field. A comprehensive overview of the field in its current state is given in a very recent review by Foreman *et al* [29].

Solid WGM resonators differ in a number of key respects from liquid ones: they are environmentally stable; offer more flexible coupling mechanisms; can sustain more straightforwardly surface particulates; can have their external environment changed more easily; and can be produced in far more controlled ways than droplets, with a wider range of shapes possible. As such they offer great flexibility and while embedding objects within solid WGM resonators is in most cases redundant, they can also be made to act as lasers [30], [31], [32], with recent reports showing lasers made from microspheres as small as $10\mu m$ [33]. This enables a much wider range of materials to be used, in principle, for solid WGM lasers. The production of a laser results in a narrowing of the cavity linewidth, giving a higher Q than in a passive cavity. Other shapes of laser are readily produced [34], [35]: a recent review on the topic was carried out by He *et al* [36].

The focus of work on WGMs has been on sensing, and they have been used to examine the detection of biomolecules, viruses and other small particles [37]. As an example, Vollmer, Arnold and King [38] made use of a microsphere to detect the real time presence, in a label free manner, of a single Influenza A virus. The binding of the virus to the 80 μm diameter sphere, which was acting as a WGM resonator at the time, leads to to a wavelength shift in the mode structure. The sphere is produced from a tapered fibre tip and is placed into a solution containing the particles to be detected. The interaction of the internal evanescent field within the cavity and an external particle leads to a drop in energy inside the cavity. As there must be a conservation of the number of cavity photons, there has to be an accompanying frequency shift, given by:

$$\hbar\Delta\omega_r \approx -\frac{\alpha_{ex}}{2}\left\langle E(r_v,t)^2\right\rangle \tag{12}$$

where α_{ex} is the isotropic excess polarisability and $\langle E(r_v,t)^2\rangle$ is the time average of the field at the external particle's position $\boldsymbol{r_v}$due to a singe photon resonant state. The mass and volume of the detected particles can also be inferred from these techniques.

Similar approaches can be used for detection of proteins [39] and adsorption kinetics, both in passive [40] and active cavities [41], as well as cancer biomarkers [42].

Other applications include temperature sensing [43], with resolution at the nanoKelvin level [44] possible, making use of the different shifts in the TE and TM modes within the cavity to actively stabilise the temperature. Pressure sensing can be achieved,using, for example, hollow microspheres [45] or, more sensitively, using an external membrane transducer [46]. Sensing of external fields, through effects like electrostriction [47], and their perturbation of the cavity modes, can be carried out with high sensitivity: $900\mu m$ PDMS (polydimethylsiloxane) spheres can be used to detect applied fields of less than 10kV/m, with theoretical values for spheres filled with water at around 500V/m.

Force sensing is another big area, often through the optomechanical coupling between the cavity modes and mechanical resonances of the cavity or a external source. With cryogenically cooled cavities, displacement sensitivities of 10^{-19} m/Hz$^{1/2}$ have been reported [48], with room temperature force sensitivities of 74aN/Hz$^{1/2}$ with stabilities of less than 1% over one minute [49]. This latter example makes use of an external nanomechanical beam coupled to a silica microdisk resonator.

Gas sensing is also an important application area for sensitive WGM devices. Adsorption on to surface coatings is one method used to shift the resonances, and this can be used to create humidity sensors [50], along with detecting ethanol [51], hexane [52], water [53] and other vapors [54, 55]. Changes in the surrounding refractive index can also be used to produce resonance shifts for detection [56] (a technique applicable for liquid samples too [57]), while chemical changes in dopants in the sensor cavity can also be used to detect, for example, hydrogen [58].

As will become clear the scope of solid WGM sensing (and hence real world applications) far outstrips those of their liquid counterparts.

2. Droplet Lasers

We now turn to, and concentrate on, WGM lasers that are made of liquid. In what follows we will touch on the basic experimental setup for the vast majority of the experiments to date, and discuss the development of the primary dye based laser droplets, before examining some of the more niche laser areas including biologically based lasing droplets, and important emerging areas such as liquid crystal droplet lasers.

2.1. Experimental Considerations

It is worth considering the seminal paper [13] from the Chang group demonstrating the first droplet laser in a little detail, as the basic principles are common through much of the subsequent work. While the sophistication of the sources and detectors has improved, the general concept is the same in almost all cases.

Much of the Chang group work on laser droplets made use of a falling stream of

droplets, made using a vibrating orifice droplet maker. Such a device is capable of making monodisperse droplets - in this case ethanol droplets of $60\mu m$ in diameter. This is estimated to be constant to 1 part in 10^4 over a period of minutes. The orifice vibrates at 62kHz which results in a droplet being produced every $16\mu s$. This results in a large number of droplets with which to carry out experiments, but effectively means that each laser droplet is a single shot device. Other methods for making droplets include coagulation on a wire [59], resulting in droplets in the 100s of micrometer range and nebulizers [60] which produce droplets typically in the sub-ten-micrometre diameter range when designed for medical applications.

The pump beam in this first experiment was a continuous wave Argon-ion laser operating at 541.5nm. In later experiments it is much more usual to use a pulsed laser, generally a Q-switched frequency doubled Nd:YAG laser operating at 532nm. Such wavelengths in the green are well matched to common fluorescent dyes. In [13] the dye used is Rhodamine 6G (the rhodamine family of dyes are a popular choice for laser droplets). The pump light is focused to a spot a little more than three times the droplet diameter ($200\mu m$). Emitted light from the falling droplets is then collected at 90° and 0° to the pump, and analysed using a spectrograph (the 90° light) and a photomultiplier (the 0° light after filtering from the pump). This dual set-up enables the spectral output as well as the temporal behaviour and threshold properties to be probed for a single droplet, although systems with spectrographs and cameras are perhaps more common now [61]. Typically these kinds of setups will observe WGMs, but for relatively large droplets these are eliminated, e.g. as observed in [62].

The transition from simple fluorescence to lasing is shown in figure 2, while the key change in intensity as a function of pump power is shown in figure 3.

Figure 2 about here

Figure 3 about here

In this experiment the laser threshold intensity is found to be $\sim 35 W/cm^2$, orders of magnitude lower than for similar dye in a conventional dye laser; the laser output occurs at wavelengths roughly between 595 - 605nm, overlapping with the WGMs of the cavity, and shows evidence of relaxation oscillations. Note that for a dye laser droplet the threshold can be calculated using [63]:

$$\gamma_{th}(\lambda) = \frac{\frac{2\pi n_l}{n_T \lambda Q} + \frac{\sigma_{abs}}{n_T} + \sigma_a(\lambda)}{\sigma_a(\lambda) + \sigma_e(\lambda)} \tag{13}$$

where, γ_{th} is the threshold fraction of exited molecules needed for laser action at the wavelength λ; σ_{abs} is the absorption loss of the absorbing dye; n_T is the number of dye molecules per unit volume; while σ_a and σ_e are the stimulated absorption and stimulated emission cross sections of the dye. Q is the cavity Q-factor (eqn (5)).

The types of dye used in laser droplets are fairly limited. They are typically pumped at 532nm. Some of the properties of the most common are listed in Table 1. Note that Nile red's emission properties change as a function of the solvent used. Some further information on droplet laser thresholds is given in [64].

Table 1: Properties of common laser dyes used in laser droplets

Dye	Typical Pump	Typical Emission bandwidth	Emission Peak
Rhodaamine 6G	532nm	558-588nm	567nm
Rhodamine 640	532nm	611-662nm	621nm
Rhodamine 560	532nm	541-583nm	563nm
Rhodamine B	532nm	586-613nm	590nm
Fluorescein 548	532nm	540-575	548nm
Nile red	532nm	565-657nm	-

A final note is on the coupling of light into droplets: as outlined above this typically takes the form of free space coupling, but evanescent coupling via tapered fibres is also possible [65, 66]. Evanescent coupling in this way is very common for solid cavities, but obviously is more challenging for droplets.

2.2. Gain Media and Laser Types

Reviewing the literature on laser droplets highlights that the demonstration of the concept is the main focus, but work can be sub-categorised according to the type of gain media or the gain mechanism. Gain can be achieved through using conventional dyes, or through processes such as FRET (Förster resonance energy transfer) or the presence of quantum dots. Here we overview the different types of gain media and laser types. The following section deals with the technological approaches to handling droplet lasers.

2.2.1. Fluorescent dyes The bulk of work carried out on laser droplets has made use of common fluorescent dyes. Much of the initial work in the field is encapsulated in the major work by Richard Chang's group [67] examining the liquid-air interface formed by the droplets. This work uses the same basic set-up as [13] but the switch is now made to the more common nanosecond pulsed lasers in more contemporary work. The dyes used are rhoadamine 590 or rhodamine 640. Colour photographs taken of the falling droplets highlight that the excitation light is only visible at the front and back surfaces. This is due to the fact that the excitation is illuminating the whole droplet and undergoes focusing as it enters. The laser emission is seen to occur only around the circumference of the droplet at the liquid air boundary, confirming that the intense field needed to meet laser threshold conditions is satisfied at the cavity edge. Also highlighted is the extension of earlier work looking at WGMs and fluorescent spectra [68] to make use of laser output, and an important confirmation that the droplets need not be spherical for lasing to be obseved.

This latter point is analyzed in more detail by considering chaotic ray dynamics in the droplets [69]. This work examines the properties of a droplet laser as a partially closed chaotic resonator and how the properties change as the droplet deforms. Mode

splitting via deformation leads to refractive loss and hence the Q is degraded. In the spherical limit loss is minimal, but where loss occurs, the Q is significantly impacted. The point of the escape of the field corresponds to a process called the "Kolmogorov-Arnold-Moser(KAM)/Lazutkin transition" which is the point where a Hamiltonian system transitions to chaos. The theory explains the different patterns of light seen in prolate and oblate deformed droplets.

The early Chang group work is clear in demonstrating a number of phenomena but does not probe the details. The work of Lin *et al.* [70] started to broaden the discussion, also using Rhodamine 590, but this time dissolved in water to minimise the mode competition from stimulated Raman scattering (SRS), by effectively suppressing the SRS threshold compared to that found in ethanol. Using an accurate measure of the threshold intensity they calculate a Q value for the cavity of $\sim 10^4$. Other firsts include the first detailed assignments of the mode features, with a consideration of the appearance of TE and TM modes, demonstrated by the modes after polarisation filtering. This is followed up in considerably more detail in later work by the same group [25, 71]. Also addressed is a more general consideration of the laser emission, looking at the angular properties. This leads to the conclusion that the droplet has a wide range of emission regions all formed round great circles within the sphere with their own orientation.

Biswas *et al.* were the first to look at the details of the temporal behavior, with Rh 6G in either water or ethanol. Of note is the fact that the laser emission has a faster rise time than dye solution in the bulk phase and compared to SRS phenomena. They offer some explanation for this latter point, in that the absorption is higher in dye doped droplets, meaning a longer time is needed to build up the resonances that support SRS, as well as the fact that lasing and SRS may couple to the same mode, resulting in competition and hence some delay. The study also suggests that such lasers can show relaxation oscillations, a point which is discussed, with a calculation of the period of relaxation, in more detail in [72].

In [73] the effect of pump power and laser dye concentration are studied. As these are increased the laser peak linewidths are seen to increase; if the excitation beam size is altered from above the droplet diameter to below at fixed power then the spectra show more complex structure, explained as possibly being due to different coupling efficiencies to different mode orders.

Other pumping mechanisms were examined in this early period of work, with the Chang group exploring two-photon pumping [74]. Courmarin dye as well as Rh 6G was explored, dissolved in ethanol. The pump source for Courmarin was a pulsed 532nm source, passed through a Stokes shifted gas cell to enable pumping at 629.9nm, with the laser emission then at 455-460nm, while a pulsed 1064nm laser was used as the two-photon pump for the Rh 6G in ethanol. Lasing using fluorescent dye (DASPI) under two-photon excitation was also demonstrated [75].

As well as exploring pumping options, a consideration of the effect of adding things other than dye molecules into the droplets was needed - the first example was provided

by Armstrong *et al* [76]. In this work the ethanol droplets were doped with fluorescein 548 dye as well as a sol (a colloidal suspension of very small particles in a liquid) made from sub-micron polystyrene spheres in the range 25-500nm. These particles are doped with a red dye. The excitation beam pumps the fluorescein which in turn emits and pumps the sol particles. Excitation peaks from the sol are not evident in the absence of the dye, and hence the conclusion is that there is a Förster energy transfer process at play. This was the first example of a FRET based droplet laser, a mechanism which will be discussed further below.

The follow up to this work [77] reported on the effect of changing the concentration of particles within the droplet (see also [78]). Here the latex particles added have no dye, and so initially act to enhance the scattering within the droplet and improve the number of modes visible. As the concentration increases the scattering loss gets higher and suppresses the laser output. For a given dye concentration in the droplet and given droplet size this suppression concentration (measured as the particle surface area) is fixed, independent of particle size. This constancy is due to FRET processes, but this time acting in a negative sense due to adsorbed dye molecules on the spheres being further away from each other than in solution. Similar work was reported in [79] looking at SRS suppression.

The presence of particles within the droplet can also impact on the spectral output of the droplet. By making use of a suspended droplet attached to a wire it is possible to probe the properties of a single droplet [80, 81]. Repeated excitation of the same droplet can lead to a blue shift in the output spectrum, due to breakdown processes within the droplet producing scattering centres, or due to the presence of nanoparticles [82], work which has interesting parallels to current studies on random lasers [83], or later work on lasing in ionic liquids [84].

Similar blue shifts can be seen for droplets when an absorber is added to the droplet in addition to the dye (increased dye concentrations lead to a red shift) [63]. As the absorber concentration increases, so does the blue shift, with bigger increases appearing when the absorption spectrum of the absorber overlaps with the fluorescence spectrum of the dye, a phenomenon that can be explained by introducing extra loss mechanisms for the presence of the absorber into standard cavity models for dye lasers. Similar effects are seen when the dye within the droplet is a saturable absorber [85].

More complex particles can also be added to the droplets with lasing being sustained. Water/glycerol droplets with Rh 6G and a fat emulsion (which is highly scattering) give enhancement of up to an order of magnitude in intensity output [86]. Droplets which would not normally lase can be made to do so by introducing the fat droplets ('Intralipid'). This work, along with follow-up work [87], make claim to be the first to make use of biological material within the laser droplet, and the suggestion is that this technique could then be used to enhance detection capability for materials such as biocolloids and biomolecules, as well as be useful in probing biological properties in vivo, work which would not be realised for a further 20 years [88, 89]. Work by the same group also explored other biomolecules, such as vitamin B2 [90] (and vitamin

A by others [91]), demonstrating lasing of a material in which no bulk material laser observation had been made.

Active colloidal suspensions have been demonstrated [92] where the droplet does not contain a gain material such as a dissolved dye, but rather fluorescent particles particles act as the gain medium. The droplets here are $100\mu m$ with a red fluorescent powder of 1-2μm acting as the emitter. The lasing threshold can then be lowered by adding in a scattering medium (the Intralipid discussed above). It is also of note that the spectral narrowing of the laser output is not perhaps what might be expected as the pump energy is increased, compared to the changes above and below threshold. It is therefore worth considering carefully what constitutes lasing in such systems, with line narrowing not being sufficient proof that lasing has occurred.

This idea of complex lineshapes is also considered in more conventional dye droplets [93] using Rh 6G or Pyrromethene in $60\mu m$ diameter water droplets. Here it is found that the spectral width is constant but then broadens when chemicals such as ethanol or DMSO are used as the solvent. The width can change by as much as 30% at high pump intensities. Using these differing solvents enables more complex feedback mechanisms with the pump, including SRS generation. These interactions, not present in water, make the output broaden, and could be due to four-wave mixing between the the laser output from the dye and the SRS peaks from the solvent WGMs, since the spectral broadening always follows SRS of the solvent.

In addition to colloidal dispersions within a droplet, core-shell 'droplets' perhaps offer more control over the physical properties of the laser. A system with a glass bead covered in a water/glycerin mixture with Rh 6G wa studied in [94]. A 7.9 micron radius glass bead is used and when the liquid shell is between 14.5 microns and 0.4 microns. The dynamics can also be probed as the layer evaporates. For the thinnest layers a 40nm blueshift in peaks and a dramatic increase in number of peaks is observed. In this experiment, the droplets are levitated in an electrodynamic balance, then the glass beads collide with them to make the laser device. The enhancement in number of peaks is possibly due to mode enhancement/reduced loss through interaction with solid core. There are issues however, due to possible core-shell interactions, which seem to increase noise in the output spectra that is not observed in the absence of the core. The blue-shift in the output spectrum is attributed to scattering by the Rh 6G precipitate.

Improvements in the technical measurements of cavity peaks, coupled with better theoretical understanding of the process and computational tools to automate mode assignments and strengths to cavity peaks started to enable more quantitative measurements to take place. In [95] these improvements were bought together to offer a detection resolution around 3cm^{-1}. Technical enhancements included better photomultiplier sensitivity as well as better detection electronics and A-to-D conversion, leading to improved detection times (from $\sim$ 1 hour to $\sim$ 8 minutes). Active feedback was also introduced to keep the droplet size constant over the acquisition period. By offering this new highly stable and sensitivity detection efficiency the mode assignments become accurate enough to then enable measurements of refractive index of the droplet,

the temperature and temperature gradients within the droplet, as well as use this information to calculate evaporation parameters such as cooling rate.

As with any laser system there will always be a need to try and improve the laser quality - whether lasing droplets need significant beam parameter improvements is a debatable point, however. One way of narrowing the laser linewidth is to use a narrow linewidth seed laser, as demonstrated in [96]. In a droplet laser, more conventional intracavity line narrowing components such as an étalon are clearly not feasible. A narrowband dye laser illuminates the droplets as well as the pump beam, with the seed laser ahead of the pump by a few nanoseconds. This delay enables the seed laser to build up in preference to modes coupled to the cavity via spontaneous emission. In this way modes from the two processes can overlap, and the seed laser can suppress modes which do not and prevent them from achieving threshold. By tuning the seed laser onto one of the cavity modes, the laser output intensity increases significantly and the linewidth narrows.

Variations on the standard dyes used in most of the laser droplets are also possible, with a notable example being the observation of a chemical laser, making use of a chemiluminescent chemical from a light stick [97]. These sticks force chemical mixtures together to produce light and are commonly seen at funfairs and fireworks displays. In the case of a laser droplet the chemiluminescence process produces an excited dye molecule which emits light. This internal production of light is sufficient to uniformly pump the droplet and produce laser output. The threshold of the system can be determined by adding in absorbing material into the droplet to suppress the output. In this case the droplets are fairly large ($\sim$2mm radius) and are produced as pendents by forcing the liquid through a capillary where the droplets hang from the end. In the case of a pendant emitter the emission intensity of the laser changes as the point at which the measurement is made at different latitudes on the droplet. Since the pumping is uniform this suggests that the variation in surface curvature at different latitudes leads to changes in the output leakage rate. Pendant droplets are also considered in [98], and used to enable frequency locking to a WGM in [99].

2.2.2. Quantum Dots With work being carried out on active particles within a droplet to provide laser gain [92] it seems obvious to put slightly more interesting particles inside to see what can happen. Quantum dots (QDs) are highly topical at present both in laser media but also as biological tags and markers. The first work to make use of QDs placed nanocrystal CdSe/ZnS particles into electrodynamically trapped water/glycerol droplets (the glycerol, as in many of these types of experiments, helps to control evaporation of the droplet) [100]. The droplets were around 10-40μm in diameter and pumped with a 532nm nanosecond laser. Multimode and single mode lasing is observed, depending on the droplet size; high pump powers induced small amounts of droplet evaporation and blue shifts in the output spectrum are observed. The pump laser also has an effect on the droplet position within the trap, meaning extra control is needed to stabilise the position to the micrometer accuracy needed, but Q values of at least 6.5×10^3 are still

measured. This work was extended by Iftiquar *et al* [101, 102] who considered similar droplets and quantum dots, again making use of a Paul trap to capture the droplet with QDs and rhodamine dye added. The system was used to make estimates of the emission cross section of the QDs, and also demonstrates the stability of the droplets using ultra high speed imaging.

The ability to use QDs within droplets could be taken much further with the development of stabilized emulsions providing the optical cavity. Work on this has been carried out where the quantum dots form the droplet outer shell, encapsulating toluene [103] in an aqueous environment. The QDs were CdSe/ZnS and cavity Q factors of $\sim$5000 are recorded against a theoretical maximum of $\sim$9000 for $23\mu m$ spheres. QD shell layers can be used to create lasers, which has been demonstrated in optofluidic ring resonators [104], and so could possibly be extended to these new forms of Pickering emulsion. Work demonstrating the optical trapping of droplets containing QDs [105] also indicates that lasers should be possible from droplets that are not charged.

Tunable output emission using combinations of QDs and more stable output is observed for WGMs using ionic liquids containing QDs under cw pumping (but not laser output) [106], offering new options for lasing tuning. Ionic liquids are less prone to evaporation than typical glycerol/water mixtures and may improve QD output properties [107].

2.2.3. FRET Lasing FRET [108, 109] based lasing is interesting in that it might enable real world applications in biosensing for laser droplets. FRET works through an acceptor molecule being excited by the pump laser and then transferring this energy over to an acceptor molecule which emits through fluorescence. The molecules must be very close for the process to activate and is widely used in exploring dynamic processes in, for example, protein interactions. The first example [77] of direct interest here was one of the earlier works in the field, and has been applied in microfluidic systems [110] (including non-droplet based optofluidic ring resonators [111, 112]) and on superhydrophobic surfaces [113] using both conventional dyes as well as labelled DNA complexes [114].

2.2.4. Biologically active media As discussed in subsection 2.2.1 there was a range of early work making use of biological or biologically inspired material to produce droplet lasers [92, 90, 115, 86, 87]. A small jump in terms of practicality and functionality was made in [116] with the introduction of a superhydrophobic surface (a modified PLLA surface with a contact angle of 157°) to hold the droplets, in this case a vitamin B2 derived biomolecule, flavin mononucleotide, in water/glycerol droplets, Figure 4. The bio-compatible surface can be patterned into microwells and so that many droplets can be captured simultaneously. The wells can then be capped to produce a small device.

Figure 4 about here

A different form of biomaterial lasing was demonstrated by Jonas *et al*

[60] by making use of common fluorescent proteins used in biological imaging. Superhydrophobic surfaces are loaded with droplets with the Venus yellow fluorescent protein; lasing is shown to be possible using a 488nm femtosecond pump laser. Droplet sizes are typically in the range of 3-10μm radius. This experiment makes use of a novel dye, but is fairly routine otherwise. The particular novelty lies in the secondary experiment in which the droplet is loaded with *E. coli* bacteria which are able to express the fluorescent protein, figure 5. Each droplet has 5-15 bacteria. In this way it is shown that it is possible to create a laser using a "single micron sized fluorescent bacterial cell". Lasing can have an on/off behaviour due to the bacterium moving in and out of the limited excitation volume within the droplet. Hence the method demonstrates the significant potential for using droplets as biosensors through signal enhancement, but flags up the limitations of relying on a technique where the thing being sensed must be within the small excitation region at the rim of the droplet. Whether that object is either subject to significant Brownian motion or can propel itself this offers a challenge for real world applications.

Figure 5 about here

One of the major landmarks in the field of droplet lasers over the past few years has been the use of biological material to act as the laser cavity, and the ability to produce lasers within tissue making use of this idea. The primary work comes from two publications, Humar and Yun [89] and Schubert *et al* [88]. Both focus on the development of intracellular lasers, with the ultimate goal of producing optical barcodes in the form of solid microspheres within cells. Each sphere can be uniquely identified through its WGM spectrum and so introducing such beads into cells enables cells to be tagged and tracked in fairly straightforward ways. If, for example, three beads were introduced into a single cell then if the beads all had different fluorescent dyes embedded, provided the output spectra were not overlapping, then 2×10^{11} cells could conceivable be tagged based on the subtle differences in the size of the different spheres.

In [89] there is a wider focus than on just solid microspheres. Oil droplets that are injected into cells, as well as natural lipid droplets inside cells, are considered, figure 6. PPE oil is mixed with Nile red dye to produce droplets in the range of 4-20μm that are injected into the cells. Droplets are then pumped using 5ns pulses of 535nm light, and those with diameters larger than 7μm are found to display lasing, with thresholds at the level of a few nanojoules per pulse, which is sufficiently low to not to damage the cell or lead to undue heating effects.

Figure 6 about here

One of the interesting applications of this technique is that as the laser emission spectrum is linked to the morphology of the droplet, any stress placed on the cell can be monitored by observing the output behavior. As stress is applied, the shape change leads to the lines splitting, which enables the major and minor axes of the droplet to be determined. This in turn, for small deformations, enables a stress to be calculated with

a force sensitivity of $\sim$20pNμm^{-2}.

Additionally it is possible to create an intracellular laser without the need for an external cavity to be injected into the cell. Making use of lipid droplets naturally occurring in a cell, a laser can be created. Cells from pig tissue were treated with a fluorescent dye which permeated into the lipid droplets, and the near spherical droplets exhibited WGMs and lasing. However it is possible to take this even further, and look at *in-situ* lasing. In the tissue matrix the cells are much more closely packed and so the droplets have more random shapes, which has the consequence of increasing the necessary pump power due to the lower Q factor. This can be overcome by injecting collagenase into the tissue along with the fluorescent dye, helping to release the cells from the tissue matrix, and results in more spherical droplets, lowering the threshold. The cells can then be pumped by introducing an optical fibre through a needle hole. The cells (adipocytes) near the fibre tip acted as lasers. It is also remarkable that cells outside the treated area also demonstrated lasing, removing the need for the collagenase.

2.3. Liquid Crystals

A class of droplet laser that sits apart from the much of the rest of the work discussed in this review is one that makes use of the droplet structure in a different way from spherical cavities to create a resonator, and hence does not depend on WGMs. These are liquid crystal devices and the resonator is formed due to the modulation of the refractive index within the sphere, creating a Bragg resonator that possesses the properties of a photonic band gap material. The first example of this type of system is presented in [117], figure 7. The liquid crystal material (a cholestic liquid crystal (CLC)) is doped with a laser dye with the chiral nature of the CLC enabling the Bragg resonator to be formed when dispersed in glycerol. The pump, as is standard, was a 532nm nanosecond pulsed Nd:YAG. The sample containing the doped CLC spheres is placed on a microscope slide and a single droplet is then pumped. Increasing the pump demonstrates a lasing threshold, which decreases with droplet diameter, down to $15\mu m$ in this case. The special cavity formed by the CLC gives rise to omnidirectional output of the laser, and hence acts as a point-like source, which differs from the MDR lasers considered elsewhere. Other differences include the fact that the lasing wavelength is determined by the cholesteric pitch, which in turn is tunable by temperature, and hence 10's of nanometres tuning can be achieved in a linear fashion with a gradient of around 3.5nm/K. Phototunability may therefore be possible. These types of laser, breaking away from the the need for MDRs may offer significant flexibility for future integration of such devices. As the authors state, "The proposed procedure of making a CLC onion microlaser by mechanical mixing is simple and straightforward and produces millions of microlasers in a fraction of a second."

Figure 7 about here

The same type of CLC microdroplet lasers can be further improved by adding an azo-chiral dopant [118]. The dopant changes its isomerisation as it is illuminated

with weak UV light, which has the effect of changing the interaction with the liquid crystal and altering the pitch of the CLC droplet (which, as indicated above, controls the laser output). In this way tuning over 23nm has been shown. With high intensity UV illumination the isomerisation becomes very strong and distorts the CLC structure such that laser stops. Hence the droplet laser can be turned on and off as well as tuned by simple intensity control of the illuminating light.

Further control over lasing properties arises when comparing small to large chiral nematic liquid crystal droplets [119, 120], where random lasing is observed for small droplets, while band-edge lasing, with corresponding cavity resonance properties, is observed in larger (typically greater than $10\mu m$ in diameter). Again simplicity is key, as the emulsions are made by mixing, coating and deswelling, and changes in mixing rates changes the size, enabling devices to be made that operate in the desired regime, which can be detected by examining the linewidth properties of the output. Lasing is also possible in inverted liquid crystal matrices [121].

Liquid crystal (LC) droplets can be made to act as MDR-based lasers and resonators [122], and in [123] nematic LC droplets dispersed in water are used. A single droplet is optically trapped using optical tweezers and then the output spectrum is monitored as a surfactant (SDS, sodium dodecyl sulphate) is added to the water. The LC orientation changes in response to the surfactant which has the effect of altering the output spectrum of the laser, implying that the WGMs can be used to monitor the surrounding medium with high sensitivity. The liquid crystal droplets are doped with Nile red dye, are around $14\mu m$ in diameter, and pumped with a pulsed 532nm laser.

More complex control over the laser properties and processes can be offered by creating a double emulsion with an outside layer of CLC material encapsulating an aqueous phase holding the laser dye [124]. Altering the type and combination of CLC and dye materials enables a switch between different modes of laser operation (between Bragg and MDR based lasers), due to the differing alignment of the crystal helical axes in each case. Which mode the laser is operating in can be probed by examining the temperature dependence of the laser output, as Bragg type lasing depends on this, while multimode lasing peaks that do not shift with temperature are assigned to MDR based lasing.

The fact that core shell particles, see figure 8 can be made like this implies that other particles can be inserted into the core. In [125] magnetic nanoparticles are placed into the aqueous phase in the core and this enables them to be manipulated by the application of an external magnetic field, as well as droplet arrays (for example close packed hexagonal arrays) to be formed. Again the laser output is tunable by around 50nm through temperature control. This type of active control is well suited for integration into microfluidic devices.

Figure 8 about here

Chiral microspheres made from LC material have also been shown to display lasing behaviour [126], and improvements in materials have led to photoresponsive shell core

lasers being produced [127], making use of photoisomerisation. Tuning was possible over a range of 50nm from 590nm to 640 which can be reversed by storing the particles in the dark for 12 hours - the possibility exists for combinations of materials to enable lasing over the full visible spectrum, for example.

2.4. Other

It is worth noting a few other droplet based studies that fall outside our coverage of lasers. The Chang group's early work looked at other cavity enhanced droplet possibilities, demonstrating stimulated Raman scattering (SRS), with the threshold significantly lowered due to the cavity enhancement provided by the droplet [128]. SRS was demonstrated in water as well as ethanol. This work would be the precursor for the development of Raman droplet lasers. Further studies indicating the utility of droplets as simple sensors was work examining shape distortions of falling droplets [68]. Here the droplets are illuminated with counter-propagating beams that initiate a shape oscillation, The ethanol droplets are doped with Rhodamine 6G, and the fluorescent signal is then monitored as the droplets oscillate. The morphological dependent resonances are then monitored enabling, for example, a $25\mu m$ radius droplet change in aspect ratio to be measured at the level of 0.001.

Nnonlinear effects such as coherent anti-Stokes Raman scattering (CARS) and coherent Raman mixing [129], were made possible by the enhancement factor offered by the droplet cavity. Campillo *et al* [130] offered an application for droplets to act as cavity QED enhancers, in many ways a precursor of current work in the field, with enhancements demonstrated of 120 in the emission spectrum of Rh 6G. The robustness of modern microfabrication techniques for resonators for cavity QED work [131] makes the use of droplet cavities largely redundant for sophisticated work, but this paper did lay out some of the possibilities for the field.

3. Laser Control

In this section we consider the techniques necessary to control the localisation and movement of droplets in more modern implementations of the original falling droplet experiments. The quest for practical applications of droplet lasers requires stable droplets and areas such as microfluidics, superhydrophobic surfaces and single droplet manipulation methods are bringing about significant improvements in the ultility of these fragile devices.

3.1. Optofluidics

While much of the work on laser droplets has been carried out in aerosols, the flexibility of having the droplets as part of an emulsion has many attractions - localisation is possible and parallelisation becomes plausible. Microfluidics has developed powerful techniques for the production and control of mixed phase liquids [132] and droplets

(often called digital microfluidics) [133] and is an obvious choice for new laser droplet devices.

Typically a device will make use of a T-junction, figure 9, which produces a stream of monodisperse droplets containing the laser dye. The droplets are formed in a second liquid phase. In the first work of this kind [134] the droplets are $50\mu m$ water droplets and are produced in an oil phase. The laser dye is Rh 6G or fluorescein. In this case it was found that the relative refractive index between the two phases was too low to support MDRs, so glycerol can be added to the water shifting the difference from 1.03 to 1.1, at which point MDRs are observed. The droplets stream past counterpropagating optical fibres, one of which is used to excite the laser dye, the other to collect the output.

More sophisticated techniques involve the use of multiple dyes in the droplets, as shown, for example, in [135]. The microfluidic system is similar to that used in [134] but instead uses a four way junction into which two dyes and the oil phase flow (essentially two opposing T-junctions). This enables droplets with alternating dyes to be produced in a stream with sizes ranging from 20-40 microns. The generation frequency could be varied between 25Hz and 3.6kHz. This enabled the switching of the laser emission to be as high as 3.6kHz, which is primarily limited by the speed of the droplets, faster than any dye laser at the time of the work. The dyes used were Rh 560 and Rh 640 and the the droplets formed using benzyl alcohol due to its high refractive index (n= 1.54); the oil phase was HDE-7500 with a refractive index of n=1.29, giving a high relative refractive index between the two phases. The pump was a 532nm nanosecond laser. Tuning can also be incorporated by allowing the droplets to dissolve in the bulk fluid, hence changing size: tuning over 80nm can be demonstrated in this way [136].

Figure 9 about here

An important conclusion from such work is that the one of the main limitations is the coupling of the system to large, expensive laser systems for the pump. There is a necessity to replace these with more compact components for practical work - laser thresholds could be brought down towards the levels provided by low power on-chip lasers if higher refractive index contrast between the droplet and surrounding phase can be engineered and if coupling into and out of the droplets can be improved.

Similar work [137] was demonstrated using a Fabry-Perot resonator formed by two coated optical fibre end facets that the droplets pass through. Single mode operation is observed for each of the dyes with a switching speed up to 1.28kHz.

A further level of sophistication can be introduced by controlling the position of the droplets. Kuehne *et al* [138] make use of an electrowetting technique to move droplets in and out of an excitation region. The laser cavity is formed by two of the electrodes. This digital microfluidic system has passive droplets (dimensions about 2×2 mm) placed onto the platform and then these can be moved to the point of interest, allowing droplets with many dyes to be loaded at once. Dyes with coverage over the whole visible spectrum are chosen to demonstrate the capability and are pumped by a pulsed UV source.

Alternative microfluidic strategies employ components of the chip as the optical

resonator, as in the case of optofluidic ring resontaors (OFRRs) [110]. In these types of system the droplets are produced in the microfluidic system and fed into a capillary channel. The channel cross section then acts as the resonator, and a droplet passing through the section that is being pumped will have some light coupled into it. This, along with the Fabry-Perot designs, has the advantage over conventional WGM based droplet microfluidic lasers in that the carrier and droplet relative refractive index is no longer an issue, making experiments in which an aqueous phase can be used as the laser possible: important if the goal is to carry out biological sensing. OFRR lasers also should have more stable droplet sizes, leading to more stable outputs due to the removal of shape and size oscillations. The output coupling of the light is more straightforward than with a liquid droplet as a fibre, for example, can be directly coupled to the OFRR. High Q values for the OFRR compared to droplet resonators may allow lower laser thresholds to be achieved as well (up to six times lower reported in [110]). The control possible in an OFRR can be demonstrated by using the downstream microfluidic chip to mix two dyes into single droplets. If these contain a donor and acceptor dye then by altering the concentrations it is possible to tune the output of the laser via FRET; 150nm tuning is shown in [110]. In addition to tuning this also suggests biosensing applications may be possible. OFRR, of course, offer flexibility by simple integration with microfluidics, and continuous phase flow, or even static fluid, may be more flexible than droplets for many sensing applications. Work in this area is much more widespread than droplet lasers *per se* [139, 140, 141, 142] and recent work has made use of quantum dots [104] and FRET using quantum dots as donors [112]. Use of droplets in such systems could improve the spatial control over the sensing region, but possibly not in any significant way, and the extra components needed to make the droplets may make systems unnecessarily unwieldy.

Something quite new in the field is a laser made from an array of droplets [143] in which the periodic structure formed by the droplets provides the feedback rather than the cavity formed by the droplet. The droplets in a microfluidic device form a distributed feedback (DFB) structure, figure 10. The droplets are benzyl alcohol with Rh 6G, immersed in mineral oil and are deliberately made too small to support WGMs; the cross section of the channel is about 1.5 x 5 microns. The pump is a Nd:YAG q-switched at 532nm and passes through a cylindrical lens to pump multiple droplets simultaneously, while the output is single frequency at 586nm at the initial droplet pitch. The period of the arrays can be tuned by altering the fluid pressure, which leads to tuning of the laser output over a range of about 70nm. This type of device looks plausible as an on-chip source (more so than a single droplet) that can be integrated with on-chip spectrometers.

Figure 10 about here

Droplets can also be formed and held at the interface of a liquid and air. Making use of inkjet printing Yang *et al* [144] placed a droplet of Rh6G-doped epoxy resin onto a water-air interface. This then formed a floating optical cavity that could be pumped to

form a laser. Moreover the droplet output could be tuned by altering the water surface tension by changing the surfactant concentration used. This enabled the output to be shifted around 10nm, and was seen to be bidirectional - an issue with more conventional tuning strategies for droplets. The output shift could in turn be used to sense chemical changes in the aqueous phase. As ethanol was added the interaction between the ethanol and water molecules led to a change in the surface tension and hence a wavelength shift. The theoretical sensitivity of this technique is estimated to be $\sim 6\times10^3 mol/ml$, limited by the cavity Q.

There are, of course, a much wider range of optofluidic lasers possible than those made using droplets. A good short overview of the current technology and applications can be found in [145].

3.2. Elastomers

Another way of embedding droplets into another substance is to place them into a solid matrix rather than the liquid one of microfluidics. This enables the droplet to be manipulated by the external manipulation of the matrix. In [146] work towards this end was carried out using a methanol droplet containing Rh 6G and a surfactant placed, using a needle, into an elasomer made with polysiloxane as it was solidifying. The droplet formed was approximately $60\mu m$ in diameter. The most interesting thing here is that the droplet could then be easily deformed by compressing the elastomer, figure 11. This enabled the WGMs (no lasing in this case) to be tuned over 0.4nm from a 0.03mm compression.

Figure 11 about here

By using a polymer droplet instead of an organic liquid, the stability of a laser embedded within an elastomer can be improved [147]. Different dyes enable lasers spanning over 100nm difference in output wavelength to be developed, and the same type of tuning through mechanical deformation is possible; single mode operation is found for droplets around $14\mu m$ in diameter. As elastomers (such as PDMS) remain partially in a liquid state as they harden it may be possible to integrate waveguides into the polymer to enable better output coupling from the lasers.

3.3. Droplet Formation and Localisation

Much of the earliest work on droplet lasers made use of streams of falling droplets, which limits the majority of practical applications of the technique unless the focus is on droplet dynamics. In this section we briefly review the core technologies used to provide localisation of droplets in air. These broadly fall into four categories: optical trapping, acoustic trapping, the electrodynamic balance and superhydrophobic surfaces. Each has been used to trap and excite droplet lasers with differing degrees of control.

3.3.1. Optical Manipulation Optical manipulation techniques fall into two categories: those that rely on the radiation pressure force, and those that rely on the optical gradient force, called optical tweezers. The first technique simply balances the optical pushing force to hold a particle against gravity, and can move a particle over a given distance by changing the optical power in the beam. Optical levitation was a very popular choice for studies of aerosol droplets in the first flush of such experiments [148]. It is still used in preference to optical tweezers in many cases due to the longer possible working distance and the flexibility this enables in terms of sample chambers and environmental control, e.g. [149]. The scattering force is given by:

$$F_{scat} = \frac{n_l}{c}\sigma I = \frac{128\pi^5 r^6}{3c\lambda_0^4}\left(\frac{n_r^2 - 1}{n_r^2 + 2}\right) n_l I \tag{14}$$

Optical tweezers [150] are a three dimensional optical trapping technique, outlined in figure 12, and make use of the fact that the force on a particle in the potential well formed by a focused laser beam is proportional to the gradient of the field. By focusing a beam tightly, with a high numerical aperture microscope objective it is then possible to generate a force that is able to overcome the effect of the scattering force. The gradient force is given by:

$$F_{grad} = \frac{2\pi n_l r^3}{c}\left(\frac{n_r^2 - 1}{n_r^2 + 2}\right) \nabla I \tag{15}$$

Figure 12 about here

An optical tweezers [151, 152] differs from a levitation trap in that changes in power will not alter the particle position: to move the particle up and down the focal point of the beam must be changed in some manner. Trapped droplet lasers have been demonstrated, e.g. [153]. This work made use of Rh B doped water/glycerol aerosols with diameters from around 8-11μm, and changing the droplet size resulted in tuning of the output over 30nm. Note however that optically trapping aerosols is more complex than in particles in liquid, and more consideration must be given to trapping parameters [154].

Trapping in emulsion is equally possible (and possibly offers more flexibility). Work has been carried out, as mentioned, trapping liquid crystal droplets [123], as well as more conventional dye doped droplets [155]. In the latter work one of the key points raised is the study of photobleaching of the laser dye (in this case Dil(3) in chlorofrom/immersion oil droplets). With repeated exposure to the pump the dye molecules bleach, resulting in a lower effective dye concentration within the droplet and a lowering of the self absorption within the droplet. This leads to a blue shift in the output spectrum; the photobleaching also leads to a reduction in output intensity.

Another popular technique in optical manipulation is that of optical stretching [156]. A deformable particle is trapped by the output from two counterpropagating beams and as the optical power is increased the particle deforms further, stretching along the optical propagation axis. One might expect the particle to be squashed,

deforming perpendicularly to the optical axis, but the transfer of momentum between the particle and the light is such that stretching occurs. The technique is a useful probe of the mechanical properties of soft matter, especially cells. The deformation suggests that a trapped laser droplet could be tuned. This is shown in [27], in which $50\mu m$ oil droplets doped with Dil(3) dye are trapped in water. Tuning gradients of around 0.5nm/W are reported for droplets with surfactant added, while for droplets without, and hence stiffer, the tuning gradient is of the order of 0.1nm/W. Thermally induced tuning is also observed indicating that much better thermal control is needed or that dynamic shifts in the pump position is required. The droplets also suffer from the oil dissolving, leading to a blue-shift in the output which is irreversible. Stretching techniques offer interesting opportunities, but clearly suffer from stability issues. High throughput systems might be of interest, combining the microfluidic techniques in [135] with hydrodynamic stretching techniques such as [157].

Work discussed below [22] (subsection 3.3.4) concerning droplets on superhydrophobic surfaces makes use of a tapered optical fibre to couple into WGMs in a droplet. This work makes use of a stationary droplet and a moving fibre. Making use of optical tweezers enables the opposite to take place, with a trapped droplet moved so it can couple light from a stationary fibre [66]. Quality factors in excess of 10×10^6 are measured, and may offer the opportunity for complex control of photonic circuits.

A new phase of optical manipulation is currently underway in which the microscope apparatus that is normally needed to create a trap (especially the microscope objective) is replaced by a single optical fibre. Optical tweezers can be produced in this way by shaping the end facet of the fibre [158, 159] or by shaping the beam output [160]. The ability to use fibres in this way opens up a range of possibilities for trapping in more complex environments where it is not possible to place a high numerical aperture objective, such as *in vivo* and in extreme environments such as engines or vacuum systems. In [161] a fibre is used for the first time to act as a optical tweezers for a liquid laser droplet. In this case the fibre is an 'annular core fibre' in which the trapping light travels along a annulus that surrounds a central fibre core that carries the pump light. The annulus has a cladding surrounding it, and the end facet is shaped into a cone by grinding and polishing. This focuses the light in the cladding to form an optical tweezers. DCM oil droplets of between 10 and $30\mu m$ in diameter can be trapped in water by the 980nm trapping beam and are excited by a nanosecond 532nm laser. The laser produced emits around 620nm, and as expected tunes with changing droplet size. The droplet can be moved by moving the position of the optical fibre.

3.3.2. Acoustic Manipulation Acoustic manipulation of particles is very topical [162] with a wide range of studies exploring ever more sophisticated tools to trap and move particles, particularly in liquids. With the development of phased array techniques, high frequency sources and borrowing tools and techniques from optical manipulation, acoustic manipulation offers powerful high strength trapping capabilities. Acoustic levitators are, at a basic level, very simple to produce, using a transducer and a reflector

to create standing waves. Particles can then be trapped in the nodes of the ultrasonic field, with the force exerted against gravity given by:

$$F_u p = V \rho_{liquid} g = -\nabla \rho \tag{16}$$

where V is the droplet volume, ρ_{liquid} is the droplet liquid density and p is the pressure field generated by the standing wave. As such this is another form of gradient trap; indeed a single beam acoustic gradient trap has recently been demonstrated [163].

Applying many of the more modern techniques to aerosols can be challenging however due to impedance matching issues from the transducers into air, or because the acoustic fields are generated via surface wave mechanisms, or the necessity for high frequency sources to trap very small particles. However very simple devices can be made to localise particles using standing wave geometries.

The first work to levitate a laser droplet made use of the type of standing wave resonator shown in figure 13 [164]. It consists of a transducer and reflector. The wavelength of the source was 6mm, which acts as the limiting size for the droplets that can be trapped. Droplets of 750nl (radius 5.6mm) were produced using an piezo droplet dispenser adding many droplets to get to the desired size. The droplets were ethylene glycol with Rh 6G at a concentration of 0.02M, pumped with a nanosecond 532nm laser (at 10Hz repetition rate and 5ns pulses). The laser threshold was 0.5W. The behaviour in this case was much the same as in previous work where the droplets were falling, but the localisation enabled the same droplet to be probed multiple times, and more or less identical droplets to be probed sequentially, producing multimode lasing that is easy to reproduce.

Figure 13 about here

3.3.3. Electrodynamic Balance The use of ion traps, or electrodynamic balances (EDBs), such as Paul traps [165], are limited to droplets which have charge, so are not suitable for neutral particles. It is straightforward in many instances to charge particles produced through electrospray or inkjet nozzle techniques. Ion traps offer flexibility in terms of optical axis to the particle, easy (and sometimes necessary) environmental control, and sufficient strength to trap a particle ejected from a high velocity stream, such as those coming from inkjet nozzles. This is something that is more challenging to achieve using optical trapping.

A typical EDB is made from a set of ring electrodes which are attached to an AC source. This produces a 3D pseudopotential with a potential minimum capable of holding a particle against gravity. Endcaps attached to a DC source can then be used to fine tune the trapping position. EDBs have been used for a number of lasing droplet studies by Tona *et al*, exploring the structure of the laser modes [166], the polarisation properties of the laser emission [167] and how the modes are affected by changes in laser dye concentration [78]. Lasers containing quantum dots have also been trapped in this manner [100].

3.3.4. Superhydrophobic Surfaces The early work on laser droplets clearly indicated that there was no strict requirement for the droplets to be perfectly spherical, examples being shape oscillating falling droplets and pendant droplets. The simplest form of localisation would be to place a droplet on a surface, but the wetting properties of the kinds of liquids typically used for lasers means that any form of cavity within the liquid is unlikely to be formed. This problem can be solved by placing the droplets on appropriately superhydrophobic surfaces which can support nearly spherical droplets. In this way Kiraz *et al* [168] were able to produce a tunable optical cavity by environmental control of the droplet chamber, hence altering their size. The surface was created by spin coating surface treated silica nanoparticles onto a glass substrate. The droplets were produced with a simple ultrasonic nebuliser and had typical sizes in the region of $10\mu m$ with a calculated contact angle of around 150°. Cavity Q's of more than 8000 were measured and the WGMs could be tuned of the order of 9nm. This technique can also be combined with electrowetting to enable electrically controlled tuning of the cavity spectrum [169].

This work was carried out in parallel to further work from the same group [170] looking at lasing from such droplets using water/glycerol droplets of 11-15μm radius. The droplets have no dye in them and act as Raman lasers, in the glycerol Raman band. A Q-switched Nd:YAG at 532nm is used as the pump. Using small ($\sim$11μm diameter droplets) the Q is $\sim$2000 and only cavity enhanced Raman scattering is observed, no lasing is present. For slightly larger droplets, say 12.4 microns, there is clear lasing enhancement in the droplet, see figure 14. Slight differences present here in comparison to the free space droplets include issues with heat dissipation through the surface and the ability to make the same droplet lase over and over again. This leads to on/off lasing behavior, which could be improved via better environmental control, saturating the background with nitrogen to improve the evaporative colling efficiency.

Figure 14 about here

The blinking dynamics in Raman lasing of water/glycerol droplets is also considered in [171]. Here the droplets are around 10 to 45 micrometres in diameter and reside in an electrodynamic trap. The laser stability is not good due to on/off blinking caused by thermally induced density fluctuations, evident in both single and multimode output. The blinking is found to increase when the evaporation rate of the droplet increases.The implication is that the blinking is caused by double resonances (points where the pump and laser fields are in resonance) in the evaporating droplet, which can then be altered by controlling the evaporation rate.

By adding water to the droplet the evaporation rate increases as well as the blinking burst frequency. Increasing the pump fluence also increases the evaporation rate and has a similar effect. That this works, supports the idea that the lasing heats the droplet and forces it to evaporate.

Coming back to the initial sequence of surface based work, the final core demonstration is a conventional dye based laser, using Rh B in the water/glycerol

mixture [172]. The droplets are a few microns in diameter up to around 20 and supported both single and occasionally multimode lasing.

Temperature control in these surface droplet systems is perhaps simpler to achieve than in levitated droplet or falling droplet systems, and in [173] external, active, temperature control is used to lock the droplet size enabling prolonged lasing from a single droplet, operating for up to 25 minutes, more than a thousand times longer than any systems to that point. The droplets are water doped with KCl salt and excited by a pulsed 532nm laser to produce a Raman laser. At the same time a continuous wave 1064nm laser is focused at the centre of the droplet to enable heating control. This allows photothermal tuning of the droplet size, and enables the size to be brought into resonance with the green laser, and resonant absorption of the green light triggers a self-stabilization process [174, 175, 176]. This maintains the size of the droplet throughout the experiment, and works when the resonant size of the droplet is approached by the larger droplet as it evaporates. The rate of evaporation will accelerate due to resonant heating and the droplet will then move past the resonant point and an instantaneous laser is observed. However if the droplet approaches the resonant point from a smaller droplet (from below) the resonant heating acts against any size change by decelerating the condensation rate as the droplet grows. In turn this same process acts to accelerate the condensation rate where the size decreases. This produces a stable, locked, operation point if the resonant point is found by decreasing the input IR laser power and allowing the droplet to grow until locked. Hence a droplet can be locked to a resonant point through photothermal control, and is a key component of practical devices for the future.

It is also worth pointing out that droplets sitting on a surface become fairly straightforward to probe with high precision. In [22] large 100-200μm droplets have light coupled into them using a tapered optical fibre. A narrowline width laser (<300kHz) is then scanned to probe the droplet. Q values of the order of 10^6 can be measured for such droplets, which are stable over periods of an hour; higher values may be possible to observe if observed shape fluctuations, induced by thermal processes can be better controlled.

4. Applications and Outlook

The first review of aerosol characterisation using whispering gallery modes [17] outlines the core application areas of these techniques, probing key aerosol properties such as size, surface tension, viscosity, chemical composition and evaporation. However it is fair to say none of these measurements relies on the droplets acting as lasers, simply that the droplets act as high enough quality cavities to excite WGMs. Work looking at droplet coagulation confirms this fact - early work looking at merging laser droplets [177] has largely been superseded by cavity enhanced Raman spectroscopy [178]. This work is very valuable, and has made significant impact in the study of aerosols [179], but is no longer dependent on lasing. Microchemistry too is perhaps more practical using Raman spectroscopy over laser emission analysis. [180, 181].

Other interesting work that falls into this category examines evaporation dynamics and burning rates of alcohols [182]. The study dopes the droplets with Rh 6G and then measures the cavity peaks to determine the droplet size. The measurements can, for example, ascertain that droplet evaporation is altered in the presence of other droplets, but the measurements come with the need to dope the droplets and illuminate with a nanosecond laser. Earlier work also outlines how WGM analysis can be used in this field [17]. WGM enabled lasing is not always desirable however, and in [183] the dyes used are changed to prevent lasing as this can obscure fluorescence measurements designed to measure droplet temperature.

One could argue that some of the work looking at aerosol sprays falls into a true application category, but with modern imaging techniques measurement of WGMs in such examples is perfectly plausible, although lasing does offer advantages in terms of output signal in a similar manner to the barcoding techniques recently pioneered for labeling cells [88, 89]. However, such demonstrations were made decades ago and have never really been taken forward. Is droplet lasing doomed to progress as a technical innovation seeking a solution?

More practically it would be useful to explore droplet dynamics in a high-throughput manner, and for many types of experiment the use of sprays would be beneficial. This shifts us away from the arguments for, and advantages of, localisation but enables large numbers of droplets to be processed simultaneously with very high precision. In work from Koç and Yale Universities [184] 2D images of Rh 6G doped water droplets were taken by pumping droplets from a spray nozzle using a nanosecond 532nm laser. Depending on the size of the droplets and their ability to support WGMs they either lased (with a characteristic double lasing spot) or for smaller droplets simply fluoresced. The difference in output colour clearly demonstrated which process was occurring. The technique works well for larger droplets, and the observed size distribution was 69.7 μm with a standard deviation of 23.1μm. The technique is able to offer high temporal resoltuon, ultimately limited by the pulse duration of the pump, but is limited in use for aerosol sprays with small size distribution due to limitations in coupling to MDRs. Following individual droplet dynamics (and hence evaporation) in such a system is difficult, but could be explored using holographic microscopy [185, 186].

In more recent studies in these areas, droplet evaporation dynamics can be probed using high magnification microscopy, coupled with particle manipulation techniques [187], enabling single particles to be studied. Future work could push these techniques towards combustion without the need for droplet lasers [188, 189].

So if the initial outlook for droplet lasers has in many ways been superceded, what now for the technology? The principle arguments for droplet lasers as opposed to solid WGM resonators are that they are facile to make, have dynamic properties and that they enable particles to be placed inside the cavity. They can also interact with other particles in more complex ways than solid cavities can. Laser droplets in air, perhaps, offer little real sensing capability over using solid particles or other techniques. The ability to generate droplets in emulsions, making use of microfluidics will be key for the

development of the technology, and for biosensing applications if these are to come. One area where simple sensing has been shown is through the use of FRET encapsulated within droplets - the application of the FRET signal using the laser cavity is seen to be a useful technique raising the signal to noise ratio. However until a strong demonstration of this technique is made showing molecular detection not possible using conventional techniques the development of the area remains limited. Better interaction between groups working on lasers and biological scientists is perhaps called for in targeting specific sensing goals. It also remains an open question if the use of droplets as biosensing cavities offers significant advantage over, say optofluidic ring resonators integrated with a microfluidic system. Areas such as biological lasing look interesting for a number of applications, especially in labelling large numbers of items and in particle tracking, but the outlook for droplet lasers in these areas is limited, although developing laser droplets for in-vivo mechanical stress sensing is plausible.

Perhaps the most interesting development in recent times has been the development of liquid crystal lasers, which offer a more robust droplet than their, typically, aqueous phase counterparts. These hybrid droplets could enable sample encapsulation for sensing applications, but would not enable fusion style droplet chemistry. Moreover the basic physics of the liquid crystal resonators, with different modes of optical entrapment, make them suitable for a wider range of tools, as well as offering a new route of study in their own right. They offer simple integration into microfluidics, tunable and controllable outputs, and should be simple to turn into devices with multiple droplet outputs. There remains much to be done to make sensors, but the potential is there.

4.1. Challenges and Future Improvements

The challenges that droplet lasing face, in many respects, mirror the advantages they offer: they are made of fluid, making them tunable and easily made and manipulated, but this in turn makes them difficult to handle, and their environment has to be stable, if stable output is desired. They are very small and so can be integrated into miniature devices, but this severely limits their output power, which means they struggle to offer useable outputs, limiting their applications to using induced changes in cavity modes. The major challenge that such techniques face however is simply that by using alternatives with solid cavities, much the same target applications can be realised, and realised with much higher sensitivity and precision.

If droplet lasers and resonators are to gain more traction, clearer application goals need to be developed, methods for reducing the pump requirements need to be explored and more flexible manipulation techniques need to be implemented. Droplet stability can be controlled, and indeed, instability can be exploited, but there is still room for improvement: better emulsion technology and liquid crystals will help here. The development of improved single droplet manipulation tools such as optical fibre based tweezers [161] should also help, and more sophisticated beam shaping tools [190] continue to be developed. These methods will open up new options in the development of sensors

in extreme environments, for example, probing droplet dynamics in engines, or in-vivo. Applications such as, studying drug delivery to the lungs, while speculative, might be plausible with such improvements.

Other advancements that would be useful are better methods of coupling, which play a role in some of the above. The demonstration of fibre based coupling [66] is significant in this regard - this method is heavily used by the solid whispering gallery mode community, and may offer new flexibility in controlled coupling, and enable studies to be carried out between multiple droplets [191], as well as connected droplets [192]. Very recent work has made use of this technique to produce a new class of lasers - ripplon lasers [193] - in which Raman class lasers are made using capilliary waves in an optically trapped droplet. Methods making use of elastomers would seem to offer the best chance of high parallelization, with microfluidics offering the best option for high throughput control.

4.2. Conclusions

Droplet lasers have a rich history that can be traced back to the beginnings of the field of laser technology and continue to evolve as the tools capable of measuring and sustaining droplet properties improve. They look set to continue to have an interesting future, but one which probably lies some way from the original aerosol based devices first demonstrated by Richard Chang. In nearly all aspects the current dye based laser droplets are identical to those first shown by Chang's group - the methods of production may have changed a little, and the ability to localise droplets has clearly improved, but there seems little scope to really move past the fundamental block on producing useful amounts of light from such a small cavity with limited gain. There remains lots to be optimistic about however. New developments have arisen in the past five years or so, with liquid crystal lasers, biological lasers and much improved integration with microfluidics; trapping and manipulation techniques continue to advance well beyond this sphere, and these tools have widespread portability. The field would benefit substantially through better collaborations with the life sciences, and it is clear that compelling applications have yet to develop in any substantial way.

There remains much to be done within the field, and hopefully this review can help to provoke some discussion of how to better develop the technology and look for stronger applications. As the number of papers in the broader area of droplet resonators shows good growth [64], there is a lot of hope that the technology will develop to the point where use of droplet lasers becomes routine.

References

[1] T H Maiman. Stimulated Optical Radiation in Ruby. *Nature*, 187(4):493–494, 1960.

[2] C G Garrett, W Kaiser, and W L Bond. Stimulated Emission into Optical Whispering Modes of Spheres. *Physical Review*, 124(6):1807–1809, 1961.

[3] Shancheng Yang, Yue Wang, and Handong Sun. Advances and Prospects for Whispering Gallery Mode Microcavities. *Advanced Optical Materials*, 3(9):1136–1162, August 2015.

[4] Lord Rayleigh. Cxii. the problem of the whispering gallery. *Philosophical Magazine Series 6*, 20(120):1001–1004, 1910.

[5] Lord Rayleigh. Ix. further applications of bessel's functions of high order to the whispering gallery and allied problems. *Philosophical Magazine Series 6*, 27(157):100–109, 1914.

[6] R D Richtmyer. Dielectric Resonators. *Journal of Applied Physics*, 10(6):391–398, June 1939.

[7] P Walsh and G Kemeny. Laser operation without spikes in a ruby ring. *Journal of Applied Physics*, 34:956, 1963.

[8] Arthur Ashkin. Acceleration and trapping of particles by radiation pressure. *Physical Review Letters*, 24(4):156–159, 1970.

[9] A Ashkin and J M Dziedzic. Optical levitation of liquid drops by radiation pressure. *Science*, 187(4181):1073–1075, March 1975.

[10] R. Thurn and W. Kiefer. Raman-microsampling technique applying optical levitation by radiation pressure. *Appl. Spectrosc.*, 38(1):78–83, Jan 1984.

[11] A Ashkin and J M Dziedzic. Observation of Resonances in the Radiation Pressure on Dielectric Spheres. *Physical Review Letters*, 38(2):1351–1354, June 1977.

[12] A Ashkin and J M Dziedzic. Observation of optical resonances of dielectric spheres by light scattering. *Applied Optics*, 20(10):1803–1814, May 1981.

[13] H M Tzeng, K F Wall, M B Long, and R K Chang. Laser emission from individual droplets at wavelengths corresponding to morphology-dependent resonances. *Optics Letters (ISSN 0146-9592)*, 9(11):499–501, November 1984.

[14] A Chiasera, Y Dumeige, P Féron, M Ferrari, Y Jestin, G Nunzi Conti, S Pelli, S Soria, and G C Righini. Spherical whispering-gallery-mode microresonators. *Laser & Photonics Review*, 4(3):457–482, April 2010.

[15] Kerry J Vahala. Optical microcavities. *Nature*, 424(6):839–846, August 2003.

[16] M H Fields, J Popp, and R K Chang. *Nonlinear Optics in Microspheres*, volume 41 of *Progress in Optics*. Progress in Optics, 2000.

[17] G Chen, M M Mazumder, R K Chang, and J C Swindal. Laser diagnostics for droplet characterization: application of morphology dependent resonances. *Progress in Energy and Combustion Science*, 22(2):163–188, 1996.

[18] C C Lam, Peter T Leung, and Kenneth Young. Explicit asymptotic formulas for the positions, widths, and strengths of resonances in Mie scattering. *Journal of the Optical Society of America B: Optical Physics*, 9(9):1585–1592, September 1992.

[19] Petr Chyalek. Resonance structure of Mie scattering: distance between resonances. *Journal of the Optical Society of America A: Optics*, 7(9):1609–1613, September 1990.

[20] G Chen, S C Hill, M M Mazumder, Y R Chemla, A Serpengüzel, and R K Chang. Wavelength variation of laser emission along the entire rim of slightly deformed microdroplets. *Optics Letters*, 18(23):1993–1995, December 1993.

[21] H. M. Lai, P. T. Leung, and K. Young. Limitations on the photon storage lifetime in electromagnetic resonances of highly transparent microdroplets. *Phys. Rev. A*, 41:5199–5204, May 1990.

[22] A Jonáš, Y Karadag, M Mestre, and A Kiraz. Probing of ultrahigh optical Q-factors of individual liquid microdroplets on superhydrophobic surfaces using tapered optical fiber waveguides. *JOSA B*, 29(12):3240, 2012.

[23] Petr Chýlek, J. T. Kiehl, and M. K. W. Ko. Optical levitation and partial-wave resonances. *Phys. Rev. A*, 18:2229–2233, Nov 1978.

[24] Peng Zhang, Sunghwan Jung, Aram Lee, and Yong Xu. Radiation-pressure-induced nonlinearity in microdroplets. *Physical Review E*, 92(6):063033–10, December 2015.

[25] H B Lin, J D Eversole, and A J Campillo. Spectral Properties of Lasing Microdroplets. *J Opt Soc Am B*, 9(1):43–50, January 1992.

[26] Zhenyu Li and Demetri Psaltis. Optofluidic dye lasers. *Microfluidics and Nanofluidics*, 4(1-2):145–158, 2008.

[27] Mehdi Aas, Alexandr Jonáš, Alper Kiraz, Oto Brzobohatý, Jan Ježek, Zdeněk Pilát, and Pavel Zemánek. Spectral tuning of lasing emission from optofluidic droplet microlasers using optical stretching. *Optics Express*, 21(18):21380–15, 2013.

[28] J. Ward and O. Benson. Wgm microresonators: sensing, lasing and fundamental optics with microspheres. *Laser & Photonics Reviews*, 5(4):553–570, 2011.

[29] Matthew R. Foreman, Jon D. Swaim, and Frank Vollmer. Whispering gallery mode sensors. *Adv. Opt. Photon.*, 7(2):168–240, Jun 2015.

[30] K Sasaki, H Misawa, N Kitamura, R Fujisawa, and H Masuhara. Optical Micromanipulation of a Lasing Polymer Particle in Water. *Japanese Journal of Applied Physics Part 2-Letters*, 32(8B):L1144–L1147, 1993.

[31] Hiroshi Taniguchi and Shinji Tanosaki. Characteristics of whispering-gallery-mode dye lasers utilizing dye-doped solid microspheres by uv n2-laser pumping. *Optical and Quantum Electronics*, 26(11):1003–1012, 1994.

[32] F. Lissillour, D. Messager, G. Stéphan, and P. Féron. Whispering-gallery-mode laser at 1.56 μm excited by a fiber taper. *Opt. Lett.*, 26(14):1051–1053, Jul 2001.

[33] Alexandre François, Nicolas Riesen, Hong Ji, Shahraam Afshar V., and Tanya M. Monro. Polymer based whispering gallery mode laser for biosensing applications. *Applied Physics Letters*, 106(3), 2015.

[34] S. L. McCall, A. F. J. Levi, R. E. Slusher, S. J. Pearton, and R. A. Logan. Whispering gallery mode microdisk lasers. *Applied Physics Letters*, 60(3):289–291, 1992.

[35] Jin-Feng Ku, Qi-Dai Chen, Ran Zhang, and Hong-Bo Sun. Whispering-gallery-mode microdisk lasers produced by femtosecond laser direct writing. *Opt. Lett.*, 36(15):2871–2873, Aug 2011.

[36] Lina He, Şahin Kaya Özdemir, and Lan Yang. Whispering gallery microcavity lasers. *Laser & Photonics Reviews*, 7(1):60–82, 2013.

[37] Giancarlo C. Righini and Silvia Soria. Biosensing by wgm microspherical resonators. *Sensors*, 16(6):905, 2016.

[38] F. Vollmer, S. Arnold, and D. Keng. Single virus detection from the reactive shift of a whispering-gallery mode. *Proceedings of the National Academy of Sciences*, 105(52):20701–20704, 2008.

[39] S Arnold, M Khoshsima, Iwao Teraoka, S Holler, and F Vollmer. Shift of whispering-gallery modes in microspheres by protein adsorption. *Optics letters*, 28(4):272–274, 2003.

[40] Michael Himmelhaus, Sivashankar Krishnamoorthy, and Alexandre Francois. Optical sensors based on whispering gallery modes in fluorescent microbeads: Response to specific interactions. *Sensors*, 10(6):6257, 2010.

[41] Alexandre Francois and Michael Himmelhaus. Whispering gallery mode biosensor operated in the stimulated emission regime. *Applied Physics Letters*, 94(3), 2009.

[42] Adam L. Washburn, L. Cary Gunn, and Ryan C. Bailey. Label-free quantitation of a cancer biomarker in complex media using silicon photonic microring resonators. *Analytical Chemistry*, 81(22):9499–9506, 2009. PMID: 19848413.

[43] C.-H. Dong, L. He, Y.-F. Xiao, V. R. Gaddam, S. K. Ozdemir, Z.-F. Han, G.-C. Guo, and L. Yang. Fabrication of high-q polydimethylsiloxane optical microspheres for thermal sensing. *Applied Physics Letters*, 94(23), 2009.

[44] D. V. Strekalov, R. J. Thompson, L. M. Baumgartel, I. S. Grudinin, and N. Yu. Temperature measurement and stabilization in a birefringent whispering gallery mode resonator. *Opt. Express*, 19(15):14495–14501, Jul 2011.

[45] Tindaro Ioppolo and M. Volkan Ötügen. Pressure tuning of whispering gallery mode resonators. *J. Opt. Soc. Am. B*, 24(10):2721–2726, Oct 2007.

[46] M. Manzo, T. Ioppolo, U. K. Ayaz, V. LaPenna, and M. V. Ötügen. A photonic wall pressure sensor for fluid mechanics applications. *Review of Scientific Instruments*, 83(10), 2012.

[47] Tindaro Ioppolo, Ulas Ayaz, and M. Volkan Ötügen. Tuning of whispering gallery modes of

spherical resonators using an external electric field. *Opt. Express*, 17(19):16465–16479, Sep 2009.

[48] A Schliesser, G Anetsberger, R Rivière, O Arcizet, and T J Kippenberg. High-sensitivity monitoring of micromechanical vibration using optical whispering gallery mode resonators. *New Journal of Physics*, 10(9):095015, 2008.

[49] GavartinE., VerlotP., and KippenbergT. J. A hybrid on-chip optomechanical transducer for ultrasensitive force measurements. *Nat Nano*, 7(8):509–514, 08 2012.

[50] Qiulin Ma, Lei Huang, Zhixiong Guo, and Tobias Rossmann. Spectral shift response of optical whispering-gallery modes due to water vapor adsorption and desorption. *Measurement Science and Technology*, 21(11):115206, 2010.

[51] Fufei Pang, Xiuyou Han, Fenghong Chu, Jianxin Geng, Haiwen Cai, Ronghui Qu, and Zujie Fang. Sensitivity to alcohols of a planar waveguide ring resonator fabricated by a sol–gel method. *Sensors and Actuators B: Chemical*, 120(2):610 – 614, 2007.

[52] Yuze Sun, Siyka I. Shopova, Greg Frye-Mason, and Xudong Fan. Rapid chemical-vapor sensing using optofluidic ring resonators. *Opt. Lett.*, 33(8):788–790, Apr 2008.

[53] B. Bhola, P. Nosovitskiy, H. Mahalingam, and W. H. Steier. Sol-gel-based integrated optical microring resonator humidity sensor. *IEEE Sensors Journal*, 9(7):740–747, July 2009.

[54] Vittorio M. N. Passaro, Francesco Dell'Olio, and Francesco De Leonardis. Ammonia optical sensing by microring resonators. *Sensors*, 7(11):2741, 2007.

[55] Kee Scholten, Xudong Fan, and Edward T. Zellers. A microfabricated optofluidic ring resonator for sensitive, high-speed detection of volatile organic compounds. *LAB ON A CHIP*, 14(19):3873–3880, OCT 7 2014.

[56] V. D. Ta, R. Chen, D. M. Nguyen, and H. D. Sun. Application of self-assembled hemispherical microlasers as gas sensors. *Applied Physics Letters*, 102(3), 2013.

[57] Kristopher J. Rowland, Alexandre Francois, Peter Hoffmann, and Tanya M. Monro. Fluorescent polymer coated capillaries as optofluidic refractometric sensors. *Opt. Express*, 21(9):11492–11505, 2013.

[58] Mustafa Eryurek, Yasin Karadag, Nevin Tasaltin, Necmettin Kilinc, and Alper Kiraz. Optical sensor for hydrogen gas based on a palladium-coated polymer microresonator. *Sensors and Actuators B-Chemical*, 212:78–83, 2015.

[59] H Taniguchi and H Tomisawa. Simple Arrangement for Liquid-Droplet Experiments Due to Morphology-Dependent Resonances. *Review of Scientific Instruments*, 64(12):3594–3597, December 1993.

[60] Alexandr Jonáš, Mehdi Aas, Yasin Karadag, Selen Manioğlu, Suman Anand, David Mcgloin, Halil Bayraktar, and Alper Kiraz. In vitro and in vivo biolasing of fluorescent proteins suspended in liquid microdroplet cavities. *Lab on a Chip*, 14(16):3093–9, June 2014.

[61] A Braun, C Kornmesser, and V Beushausen. Simultaneous spatial and spectral imaging of lasing droplets. *Journal of the Optical Society of America a-Optics Image Science and Vision*, 22(9):1772–1779, September 2005.

[62] H Taniguchi. Time Difference in Stimulated-Emission From Fluorescent Dye-Doped Small-Size Liquid Droplets. *Japanese Journal of Applied Physics Part 2-Letters*, 32(11A):L1615–L1617, 1993.

[63] Md Mohiuddin Mazumder, James B Gillespie, Gang Chen, and Richard K Chang. Wavelength shifts of dye lasing in microdroplets: effect of absorption change. *Optics Letters*, 20(8):878–880, April 1995.

[64] Yan Wang, Hanyang Li, Liyuan Zhao, Bing Wu, Shuangqiang Liu, Yongjun Liu, and Jun Yang. A review of droplet resonators: Operation method and application. *Optics & Laser Technology*, 86:61 – 68, 2016.

[65] Raphael Dahan, Leopoldo L Martin, and Tal Carmon. Droplet optomechanics. *Optica*, 3(2):175–4, 2016.

[66] Samuel Kaminski, Leopoldo L Martin, and Tal Carmon. Tweezers controlled resonator. *Optics*

Express, 23(22):28914–6, 2015.

[67] S X Qian, J B Snow, H M Tzeng, and R K Chang. Lasing Droplets - Highlighting the Liquid-Air Interface by Laser-Emission. *Science*, 231(4737):486–488, 1986.

[68] H M Tzeng, M B Long, R K Chang, and P W Barber. Laser-induced shape distortions of flowing droplets deduced from morphology-dependent resonances in fluorescence spectra. *Optics Letters*, 10(5):209–211, May 1985.

[69] A Mekis, J U Nockel, G Chen, A D Stone, and R K Chang. Ray Chaos and Q Spoiling in Lasing Droplets. *Physical Review Letters*, 75(14):2682–2685, 1995.

[70] H B Lin, A L Huston, B L Justus, and A J Campillo. Some characteristics of a droplet whispering-gallery-mode laser. *Optics Letters*, 11(10):614–616, October 1986.

[71] J D EVERSOLE, H B Lin, and A J Campillo. Cavity-Mode Identification of Fluorescence and Lasing in Dye-Doped Microdroplets. *Applied Optics*, 31(12):1982–1991, 1992.

[72] H Latifi, A Biswas, R L Armstrong, and R G Pinnick. Lasing and Stimulated Raman-Scattering in Spherical Liquid Droplets - Time, Irradiance, and Wavelength Dependence. *Applied Optics*, 29(36):5387–5392, 1990.

[73] J C Knight, HST Driver, and G N Robertson. Effect of the pumping geometry on the half-widths of the lasing peaks observed from Rhodamine 6G ethanol droplets. *Optics Letters*, 1990.

[74] A S Kwok, J B Gillespie, A Serpengüzel, W F Hsieh, and R K Chang. Two-photon-pumped lasing in microdroplets. *Optics Letters*, 17(20):1435–1437, October 1992.

[75] M Anand, A K Dharmadhikari, J A Dharmadhikari, A Mishra, D Mathur, and M Krishnamurthy. Two-photon pumped lasing from methanol micro-droplets doped by a weakly fluorescent dye. *Chemical Physics Letters*, 372(1-2):263–268, 2003.

[76] R L Armstrong, Xie J G, T E Ruekgauer, and R G Pinnick. Energy-Transfer-Assisted Lasing From Microdroplets Seeded with Fluorescent Sol. *Optics Letters*, 17(13):943–945, 1992.

[77] R L Armstrong, J G Xie, T E Ruekgauer, J Gu, and R G Pinnick. Effects of Submicrometer-Sized Particles on Microdroplet Lasing. *Optics Letters*, 18(2):119–121, 1993.

[78] M Tona and M Kimura. Dependence of lasing modes of microdroplets on dye concentration. *Journal of the Physical Society of Japan*, 72(5):1238–1243, May 2003.

[79] J G Xie, T E Ruekgauer, R L Armstrong, and R G Pinnick. Suppression of stimulated Raman scattering from microdroplets by seeding with nanometer-sized latex particles. *Optics Letters*, 18(5):340–342, 1993.

[80] H Taniguchi and H Tomisawa. Wavelength Shifts of a Suspended-Single-Droplet Dye-Laser by Successive Laser Pumping. *Optics Letters*, 19(22):1852–1854, 1994.

[81] X Y Pu, S Zhang, C W Chan, and W K Lee. Lasing features of dye-doped pendant drops added with polymer particles: spectral blueshift and intensity enhancement. *Chinese Physics*, 11(11):1179–1183, November 2002.

[82] H Taniguchi, M Nishiya, S Tanosaki, and H Inaba. Lasing behavior in a liquid spherical dye laser containing highly scattering nanoparticles. *Optics Letters*, 21(4):263–265, 1996.

[83] W Zhang, N Cue, and K M Yoo. Emission linewidth of laser action in random gain media. *Optics Letters*, 20(9):961–963, May 1995.

[84] Valentin Barna and Luisa De Cola. Mirrorless dye doped ionic liquid lasers. *Optics Express*, 23(9):11936–10, 2015.

[85] I J Yu and W F Hsieh. Lasing spectral blue shifts of fluorescent saturable absorbing dye in microdroplets. *Chinese Journal of Physics*, 36(3):488–493, June 1998.

[86] H Taniguchi, S Tanosaki, K Tsujita, and H Inaba. Experimental studies on output, spatial, and spectral characteristics of a microdroplet dye laser containing intralipid as a highly scattering medium. *Ieee Journal of Quantum Electronics*, 32(11):1864–1873, November 1996.

[87] S Tanosaki, H Taniguchi, K Tsujita, and B Devaraj. Bio-material laser action enforced by mixed highly scattering Intralipid in microdroplet containing pigment extracted from biological tissues. *Electronics ...*, 32(16):1484, 1996.

[88] Marcel Schubert, Anja Steude, Philipp Liehm, Nils M Kronenberg, Markus Karl, Elaine C

Campbell, Simon J Powis, and Malte C Gather. Lasing within Live Cells Containing Intracellular Optical Microresonators for Barcode-Type Cell Tagging and Tracking. *Nano Letters*, 15(8):5647–5652, August 2015.

[89] Matjaž Humar and Seok Hyun Yun. Intracellular microlasers. *Nature Photonics*, 9(9):572–576, July 2015.

[90] S Tanosaki, H Taniguchi, B Devaraj, and H Inaba. New biochemical material laser emission in microdroplets using ribo-flavin and its enhancement by mixing highly scattering intralipid medium. *Optical and Quantum Electronics*, 32(2):137–145, February 2000.

[91] M Boni, V Nastasa, I R Andrei, A Staicu, and M L Pascu. Enhanced fluorescence emitted by microdroplets containing organic dye emulsions. *Biomicrofluidics*, 9(1):014126–11, January 2015.

[92] H Taniguchi, A Kurosawa, S Tanosaki, B Devaraj, and H Inaba. Lasing action of active-particles dispersed in microdroplets and its enhanced characteristics by highly scattering intralipid-10% mixture. *Optical and Quantum Electronics*, 32(2):125–135, February 2000.

[93] Anders G Knospe and Alfred S Kwok. Spectral broadening in a microdroplet dye laser. *Chemical Physics Letters*, 390(1-3):130–135, May 2004.

[94] M Essien, R L Armstrong, and J B Gillespie. Lasing Emission From an Evaporating Layered Microdroplet. *Optics Letters*, 18(10):762–764, 1993.

[95] Jay D Eversole, H B Lin, A L Huston, Anthony J Campillo, Peter T Leung, S Y Liu, and Kenneth Young. High-precision identification of morphology-dependent resonances in optical processes in microdroplets. *Journal of the Optical Society of America B: Optical Physics*, 10(1):1955–1968, October 1993.

[96] Jürgen Popp, Mitchell H Fields, and Richard K Chang. Injection seeding of lasing in microdroplets. *Optics Letters*, 22(3):139–141, February 1997.

[97] S S Chang, N B Rex, and R K Chang. Chemical lasing in pendant droplets: lasing-spectra, emission-pattern, and cavity-lifetime measurements. *J Opt Soc Am B*, 16(8):1224–1235, August 1999.

[98] M Boni, V Nastasa, A Staicu, and I R Andrei. Characterisation of Fluorescent Pendant Droplets. *Romanian Reports in ...*, 2015.

[99] R Zullo, A Giorgini, S Avino, P Malara, P De Natale, and G Gagliardi. Laser-frequency locking to a whispering-gallery-mode cavity by spatial interference of scattered light. *Optics Letters*, 41(3):650–3, 2016.

[100] J Schäfer, J P Mondia, R Sharma, Z H Lu, A S Susha, A L Rogach, and L J Wang. Quantum Dot Microdrop Laser. *Nano Letters*, 8(6):1709–1712, June 2008.

[101] S. M. Iftiquar. Levitated microdrop quantum dot and dye laser in a modified paul trap. *Journal of Optics*, 41(2):110–113, 2012.

[102] S. M. Iftiquar, Y. Wijaya, and R Dumke. Characterization of (cdse)zns core-shell quantum dots in microdrop laser cavity. *Optics and Photonics Letters*, 04(01):1–10, 2011.

[103] Tae-Jin Yim, Thomas Zentgraf, Bumki Min, and Xiang Zhang. All-liquid photonic microcavity stabilized by quantum dots. *Journal of the American Chemical Society*, 132(7):2154–2156, 2010. PMID: 20121091.

[104] Alper Kiraz, Qiushu Chen, and Xudong Fan. Optofluidic Lasers with Aqueous Quantum Dots. *ACS Photonics*, 2(6):707–713, June 2015.

[105] Yosuke Minowa, Ryoichi Kawai, and Masaaki Ashida. Optical levitation of a microdroplet containing a single quantum dot. *Optics Letters*, 40(6):906–4, 2015.

[106] Edin Nuhiji, Francois G. Amar, Hongxia Wang, Nolene Byrne, Tich-Lam Nguyen, and Tong Lin. Whispering gallery mode emission generated in tunable quantum dot doped glycerol/water and ionic liquid/water microdroplets formed on a superhydrophobic coating. *J. Mater. Chem.*, 21:10823–10828, 2011.

[107] Takuya Nakashima and Tsuyoshi Kawai. Quantum dots-ionic liquid hybrids: efficient extraction of cationic cdte nanocrystals into an ionic liquid. *Chem. Commun.*, pages 1643–1645, 2005.

[108] Harekrushna Sahoo. Förster resonance energy transfer – A spectroscopic nanoruler: Principle and applications. *Journal of Photochemistry and Photobiology C: Photochemistry Reviews*, 12(1):20–30, March 2011.

[109] David W Piston and Gert-Jan Kremers. Fluorescent protein FRET: the good, the bad and the ugly. *Trends in Biochemical Sciences*, 32(9):407–414, September 2007.

[110] Wonsuk Lee, Yunhan Luo, Qiran Zhu, and Xudong Fan. Versatile optofluidic ring resonator lasers based on microdroplets. *Optics Express*, 19(20):19668–19674, September 2011.

[111] Qiushu Chen, Xingwang Zhang, Yuze Sun, Michael Ritt, Sivaraj Sivaramakrishnan, and Xudong Fan. Highly sensitive fluorescent protein FRET detection using optofluidic lasers. *Lab on a Chip*, 13(14):2679–2681, July 2013.

[112] Qiushu Chen, Alper Kiraz, and Xudong Fan. Optofluidic FRET lasers using aqueous quantum dots as donors. *Lab on a Chip*, 16(2):353–359, 2016.

[113] E Özelci, M Aas, A Jonáš, and A Kiraz. Optofluidic FRET microlasers based on surface-supported liquid microdroplets. *Laser Physics Letters*, 11(4):045802–8, February 2014.

[114] M Aas, E Özelci, A Jonáš, A Kiraz, H Liu, C Fan, Q Chen, and X Fan. FRET lasing from self-assembled DNA tetrahedral nanostructures suspended in optofluidic droplet resonators. *The European Physical Journal Special Topics*, 223(10):2057–2062, October 2014.

[115] S Tanosaki, H Taniguchi, K Tsujita, B Devaraj, and H Inaba. Highly scattering Intralipid-10% assisted lasing from microdroplets with acridine orange dye. *Applied Optics*, 37(12):2379–2384, 1998.

[116] Sedat Nizamoglu, Malte C Gather, and Seok Hyun Yun. All-Biomaterial Laser Using Vitamin and Biopolymers. *Advanced Materials*, 25(41):5943–5947, November 2013.

[117] M Humar and I Musevic. 3D microlasers from self-assembled cholesteric liquid-crystal microdroplets. *Optics Express*, 18(26):26995–27003, December 2010.

[118] Jia-De Lin, Meng-Hung Hsieh, Guan-Jhong Wei, Ting-Shan Mo, Shuan-Yu Huang, and Chia-Rong Lee. Optically tunable/switchable omnidirectionally spherical microlaser based on a dye-doped cholesteric liquid crystal microdroplet with an azo-chiral dopant. *Optics Express*, 21(13):15765–12, 2013.

[119] P J W Hands, D J Gardiner, S M Morris, C Mowatt, T D Wilkinson, and H J Coles. Band-edge and random lasing in paintable liquid crystal emulsions. *Applied Physics Letters*, 98(14), 2011.

[120] Damian J Gardiner, Stephen M Morris, Philip J W Hands, Carrie Mowatt, Rupert Rutledge, Timothy D Wilkinson, and Harry J Coles. Paintable band-edge liquid crystal lasers. *Optics Express*, 19(3):2432–2439, January 2011.

[121] T H Dudok, V I Savaryn, A V Fechan, V V Cherpak, B Pansu, and Yu A Nastishin. Dot lasers: isotropic droplets in a cholesteric matrix, and vice versa. *Ukrainian Journal of Physical Optics*, 15(4):227–232, December 2014.

[122] T Arun Kumar, M A Mohiddon, N Dutta, Nirmal K Viswanathan, and Surajit Dhara. Detection of phase transitions from the study of whispering gallery mode resonance in liquid crystal droplets. *Applied Physics Letters*, 106(5):051101–5, February 2015.

[123] M Humar and I Musevic. Surfactant sensing based on whispering-gallery-mode lasing in liquid-crystal microdroplets. *Optics Express*, 19(21):19836–19844, October 2011.

[124] Yoshiaki Uchida, Yoichi Takanishi, and Jun Yamamoto. Controlled fabrication and photonic structure of cholesteric liquid crystalline shells. *Advanced materials (Deerfield Beach, Fla.)*, 25(23):3234–3237, June 2013.

[125] Lu-Jian Chen, Ling-Li Gong, Ya-Li Lin, Xin-Yi Jin, Han-Ying Li, Sen-Sen Li, Kai-Jun Che, Zhi-Ping Cai, and Chaoyong James Yang. Microfluidic fabrication of cholesteric liquid crystal core–shell structures toward magnetically transportable microlasers. *Lab on a Chip*, 16(7):1206–1213, 2016.

[126] Gabriella Cipparrone, Alfredo Mazzulla, Alfredo Pane, Raul Josue Hernandez, and Roberto Bartolino. Chiral Self-Assembled Solid Microspheres: A Novel Multifunctional Microphotonic Device. *Advanced Materials*, 23(48):5773–5778, November 2011.

[127] Lujian Chen, Yannian Li, Jing Fan, Hari Krishna Bisoyi, David A Weitz, and Quan Li. Photoresponsive Monodisperse Cholesteric Liquid Crystalline Microshells for Tunable Omnidirectional Lasing Enabled by a Visible Light-Driven Chiral Molecular Switch. *Advanced Optical Materials*, 2(9):845–848, May 2014.

[128] J B Snow, S X Qian, and R K Chang. Stimulated Raman scattering from individual water and ethanol droplets at morphology-dependent resonances. *Optics Letters*, 10(1):37–39, January 1985.

[129] S X Qian, J B Snow, and R K Chang. Coherent Raman mixing and coherent anti-Stokes Raman scattering from individual micrometer-size droplets. *Optics Letters*, 10(10):499–501, October 1985.

[130] A J Campillo, J D Eversole, and H B Lin. Cavity quantum electrodynamic enhancement of stimulated emission in microdroplets. *Physical Review Letters*, 67(4):437–440, July 1991.

[131] Herbert Walther, Benjamin T H Varcoe, Berthold-Georg Englert, and Thomas Becker. Cavity quantum electrodynamics. *Reports on Progress in Physics*, 69(5):1325, 2006.

[132] M Pan, M Kim, and S Kuiper. Actuating Fluid–Fluid Interfaces for the Reconfiguration of Light. *Selected Topics in ...*, 2015.

[133] Shia-Yen Teh, Robert Lin, Lung-Hsin Hung, and Abraham P. Lee. Droplet microfluidics. *Lab Chip*, 8:198–220, 2008.

[134] Melikhan Tanyeri, Richard Perron, and Ian M Kennedy. Lasing droplets in a microfabricated channel. *Optics Letters*, 32(17):2529–2531, 2007.

[135] Sindy K Y Tang, Zhenyu Li, Adam R Abate, Jeremy J Agresti, David A Weitz, Demetri Psaltis, and George M Whitesides. A multi-color fast-switching microfluidic droplet dye laser. *Lab on a Chip*, 9(19):2767–5, 2009.

[136] Sindy K Y Tang, Ratmir Derda, Qimin Quan, Marko Lončar, and George M Whitesides. Continuously tunable microdroplet-laser in a microfluidic channel. *Optics Express*, 19(3):2204–2215, January 2011.

[137] G Aubry, Q Kou, J Soto-Velasco, C Wang, S Meance, J J He, and A M Haghiri-Gosnet. A multicolor microfluidic droplet dye laser with single mode emission. *Applied Physics Letters*, 98(11):111111–4, 2011.

[138] Alexander J C Kuehne, Malte C Gather, Irwin A Eydelnant, Seok Hyun Yun, David A Weitz, and Aaron R Wheeler. A switchable digital microfluidic droplet dye-laser. *Lab on a Chip*, 11(21):3716–4, 2011.

[139] Xiang Wu, Qiushu Chen, Yuze Sun, and Xudong Fan. Bio-inspired optofluidic lasers with luciferin. *Applied Physics Letters*, 102(20):203706–4, 2013.

[140] Qiushu Chen, Huajie Liu, Wonsuk Lee, Yuze Sun, Dan Zhu, Hao Pei, Chunhai Fan, and Xudong Fan. Self-assembled DNA tetrahedral optofluidic lasers with precise and tunable gain control. *Lab on a Chip*, 13(17):3351–4, 2013.

[141] Xingwang Zhang, Wonsuk Lee, and Xudong Fan. Bio-switchable optofluidic lasers based on DNA Holliday junctions. *Lab on a Chip*, 12(19):3673–4, 2012.

[142] Y Sun, S I Shopova, and C S Wu. Bioinspired optofluidic FRET lasers via DNA scaffolds. In *Proceedings of the ...*, 2010.

[143] Avraham Bakal, Christoph Vannahme, Anders Kristensen, and Uriel Levy. Tunable on chip optofluidic laser. *Applied Physics Letters*, 107(21):211105–4, November 2015.

[144] Shancheng Yang, Van Duong Ta, Yue Wang, Rui Chen, Tingchao He, Hilmi Volkan Demir, and Handong Sun. Reconfigurable liquid whispering gallery mode microlasers. *Scientific Reports*, 6:27200 EP –, 06 2016.

[145] Xudong Fan and Seok Hyun Yun. The potential of optofluidic biolasers. *Nature Methods*, 11(2):141–147, January 2014.

[146] Mitsunori Saito, Hiroya Shimatani, and Hideyuki Naruhashi. Tunable whispering gallery mode emission from a microdroplet in elastomer. *Optics Express*, 16(16):11915–11919, August 2008.

[147] Van Duong Ta, Rui Chen, and Han Dong Sun. Tuning Whispering Gallery Mode Lasing from

Self-Assembled Polymer Droplets. *Scientific Reports*, 3:1362, March 2013.

[148] J Popp, M Lankers, K Schaschek, W Kiefer, and J T Hodges. Observation of sudden temperature jumps in optically levitated microdroplets due to morphology-dependent input resonances. *Applied Optics*, 34(13):2380–2386, May 1995.

[149] Ryan D Davis, Sara Lance, Joshua A Gordon, and Margaret A Tolbert. Long Working-Distance Optical Trap for in Situ Analysis of Contact-Induced Phase Transformations. *Analytical Chemistry*, 87(12):6186–6194, June 2015.

[150] A A Ashkin, J M JM Dziedzic, J E JE Bjorkholm, and S S Chu. Observation of a single-beam gradient force optical trap for dielectric particles. *Optics Letters*, 11(5):288–288, April 1986.

[151] Timo A Nieminen, Nathaniel du Preez-Wilkinson, Alexander B Stilgoe, Vincent L Y Loke, Ann A M Bui, and Halina Rubinsztein-Dunlop. Optical tweezers: Theory and modelling. *Journal of Quantitative Spectroscopy and Radiative Transfer*, 146:59–80, October 2014.

[152] Richard W Bowman and Miles J Padgett. Optical trapping and binding. *Reports on Progress in Physics*, 76(2):026401, January 2013.

[153] Y Karadag, M Aas, A Jonáš, S Anand, D McGloin, and A Kiraz. Dye lasing in optically manipulated liquid aerosols. *Optics Letters*, 38(10):1669–3, 2013.

[154] Daniel R Burnham and David Mcgloin. Modeling of optical traps for aerosols. *J Opt Soc Am B*, 29(12):2856–2864, November 2011.

[155] M Aas, A Jonáš, and A Kiraz. Lasing in optically manipulated, dye-doped emulsion microdroplets. *Optics Communications*, 290:183–187, March 2013.

[156] J Guck, R Ananthakrishnan, H Mahmood, TJ Moon, CC Cunningham, and J Kas. The optical stretcher: A novel laser tool to micromanipulate cells. *Biophysical Journal*, 81(2):767–784, 2001.

[157] D R Gossett, H T K Tse, S A Lee, Y Ying, A G Lindgren, O O Yang, J Rao, A T Clark, and D Di Carlo. Hydrodynamic stretching of single cells for large population mechanical phenotyping. *Proceedings of the National Academy of Sciences*, 109(20):7630–7635, May 2012.

[158] Zhihai Liu, Chengkai Guo, Jun Yang, and Libo Yuan. Tapered fiber optical tweezers for microscopic particle trapping: fabrication and application. *Opt. Express*, 14(25):12510–12516, Dec 2006.

[159] Jean-Baptiste Decombe, Serge Huant, and Jochen Fick. Single and dual fiber nano-tip optical tweezers: trapping and analysis. *Opt. Express*, 21(25):30521–30531, Dec 2013.

[160] Tomáš Čižmár and Kishan Dholakia. Shaping the light transmission through a multimode optical fibre: complex transformation analysis and applications in biophotonics. *Opt. Express*, 19(20):18871–18884, Sep 2011.

[161] Zhihai Liu, Yunhao Chen, Li Zhao, Yu Zhang, Yong Wei, Hanyang Li, Yongjun Liu, Yaxun Zhang, Enming Zhao, Xinghua Yang, Jianzhong Zhang, and Libo Yuan. Single-fiber tweezers applied for dye lasing in a fluid droplet. *Optics Letters*, 41(13):2966, 2016.

[162] Bruce W. Drinkwater. Dynamic-field devices for the ultrasonic manipulation of microparticles. *Lab Chip*, 16:2360–2375, 2016.

[163] Diego Baresch, Jean-Louis Thomas, and Régis Marchiano. Observation of a single-beam gradient force acoustical trap for elastic particles: Acoustical tweezers. *Phys. Rev. Lett.*, 116:024301, Jan 2016.

[164] H Azzouz, L Alkhafadiji, S Balslev, J Johansson, N A Mortensen, S Nilsson, and A Kristensen. Levitated droplet dye laser. *Opt. Express*, 14(10):4374–9, May 2006.

[165] Wolfgang Paul. Electromagnetic traps for charged and neutral particles. *Rev. Mod. Phys.*, 62:531–540, Jul 1990.

[166] Masahide Tona and Masahiro Kimura. Novel lasing modes observed in a levitated single dye-doped microdroplet. *Journal of the Physical Society of Japan*, 69(11):3533–3535, 2000.

[167] M Tona and M Kimura. Polarization effects in both emission spectra and microscopic images of lasing microdroplets levitated in an ion trap. *Journal of the Physical Society of Japan*, 71(2):425–428, February 2002.

[168] A Kiraz, A Kurt, M A Dündar, and A L Demirel. Simple largely tunable optical microcavity. *Applied Physics Letters*, 89(8):081118–4, 2006.

[169] A. Kiraz, Y. Karadağ, and A. F. Coskun. Spectral tuning of liquid microdroplets standing on a superhydrophobic surface using electrowetting. *Applied Physics Letters*, 92(19), 2008.

[170] A Sennaroglu, A Kiraz, M A Duendar, A Kurt, and A L Demirel. Raman lasing near 630 nm from stationary glycerol-water microdroplets on a superhydrophobic surface. *Optics Letters*, 32(15):2197–2199, 2007.

[171] R Sharma, J P Mondia, J Schaefer, Z H Lu, and L J Wang. Effect of evaporation on blinking properties of the glycerol microdrop Raman laser. *Journal of Applied Physics*, 105(11), 2009.

[172] A Kiraz, A Sennaroglu, S Doğanay, M A Dündar, A Kurt, H Kalaycıoğlu, and A L Demirel. Lasing from single, stationary, dye-doped glycerol/water microdroplets located on a superhydrophobic surface. *Optics Communications*, 276(1):145–148, August 2007.

[173] Y Karadag, M Gundogan, M Y Yuce, H Cankaya, A Sennaroglu, and A Kiraz. Prolonged Raman lasing in size-stabilized salt-water microdroplets on a superhydrophobic surface. *Optics Letters*, 35(12):1995–1997, 2010.

[174] A. Kiraz, A. Kurt, M. A. Dündar, M. Y. Yüce, and A. L. Demirel. Volume stabilization of single, dye-doped water microdroplets with femtoliter resolution. *J. Opt. Soc. Am. B*, 24(8):1824–1828, Aug 2007.

[175] Y. Karadag, M. Mestre, and A. Kiraz. Photothermal self-stability and optical bistability of single nacl-water microdroplets on a superhydrophobic surface. *Phys. Chem. Chem. Phys.*, 11:7145–7151, 2009.

[176] Marc Guillon, Rachael E H Miles, Jonathan P Reid, and David McGloin. Thermo-optical resonance locking of an optically trapped salt-water microdroplet. *New Journal of Physics*, 11(10):103041, 2009.

[177] H J Moon, G H Kim, Y S Lim, C S Go, J H Lee, and J S Chang. Lasing images from two merging ink-doped liquid droplets. *Optics Letters*, 21(13):913–915, 1996.

[178] Jason R Butler, Jon B Wills, Laura Mitchem, Daniel R Burnham, David Mcgloin, and Jonathan P Reid. Spectroscopic characterisation and manipulation of arrays of sub-picolitre aerosol droplets. *Lab on a Chip*, 9(4):521, 2009.

[179] Rachel Symes, Robert M. Sayer, and Jonathan P. Reid. Cavity enhanced droplet spectroscopy: Principles, perspectives and prospects. *Phys. Chem. Chem. Phys.*, 6:474–487, 2004.

[180] Bartholomew S Vaughn, Phillip J Tracey, and Adam J Trevitt. Laser-initiated iodine radical chemistry in single microdroplets. *Chemical Physics Letters*, 551:134–138, November 2012.

[181] Mariko Hoshino-Nagasaka, Toshihiro Isoda, Tooru Takeshima, and Jun-ya Kohno. Scanning cavity-enhanced droplet spectroscopy: Tuning of the excitation laser for obtaining a continuous Raman spectrum. *Chemical Physics Letters*, 539-540:229–233, June 2012.

[182] P J Santangelo and I M Kennedy. Droplet lasing spectroscopy applied to droplet stream flames. *Combustion and Flame*, 117(1-2):413–421, April 1999.

[183] Lionel Perrin, Guillaume Castanet, and Fabrice Lemoine. Characterization of the evaporation of interacting droplets using combined optical techniques. *Experiments in Fluids*, 56(2):29–16, January 2015.

[184] A Serpengüzel, S Kucuksenel, and R K Chang. Microdroplet identification and size measurement in sprays with lasing images. *Optics Express*, 10(20):1118–1132, 2002.

[185] Sang-Hyuk Lee, Yohai Roichman, Gi-Ra Yi, Shin-Hyun Kim, Seung-Man Yang, Alfons van Blaaderen, Peter van Oostrum, and David G. Grier. Characterizing and tracking single colloidal particles with video holographic microscopy. *Opt. Express*, 15(26):18275–18282, Dec 2007.

[186] Matthew J. Berg and Gorden Videen. Digital holographic imaging of aerosol particles in flight. *Journal of Quantitative Spectroscopy and Radiative Transfer*, 112(11):1776 – 1783, 2011. Electromagnetic and Light Scattering by Nonspherical Particles {XII}.

[187] Stella Corsetti, Rachael E. H. Miles, Craig McDonald, Yuri Belotti, Jonathan P. Reid, Johannes Kiefer, and David McGloin. Probing the evaporation dynamics of ethanol/gasoline biofuel

blends using single droplet manipulation techniques. *The Journal of Physical Chemistry A*, 119(51):12797–12804, 2015. PMID: 26633739.

[188] Sheng ji Li and Xue feng Huang. The manipulation and combustion of carbon-based micro particles by optical tweezers. *International Journal of Optomechatronics*, 9(1):35–47, 2015.

[189] Xuefeng Huang and Shengji Li. Ignition and combustion characteristics of jet fuel liquid film containing graphene powders at meso-scale. *Fuel*, 177:113 – 122, 2016.

[190] Martin Ploschner, Tomáš Tyc, and Tomas Cizmar. Seeing through chaos in multimode fibres. *Nature Photonics*, pages 1–5, July 2015.

[191] D R Burnham and D McGloin. Holographic optical trapping of aerosol droplets. *Optics Express*, 14(9):4175–4181, May 2006.

[192] David A. Woods, Christopher D. Mellor, Jonathan M. Taylor, Colin D. Bain, and Andrew D. Ward. Nanofluidic networks created and controlled by light. *Soft Matter*, 7:2517–2520, 2011.

[193] Samuel Kaminski, Leopoldo L. Martin, Shai Maayani, and Tal Carmon. Ripplon laser through stimulated emission mediated by water waves. *Nat Photon*, 10(12):758–761, 12 2016.

Figures

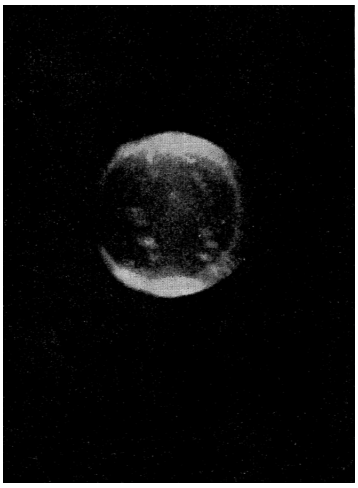

Figure 1: Photograph of the first WGM based laser made form a sphere of CaF_2:Sm^{++}. The sphere has a diameter of $\sim$ 1-2mm. The rim of the disk is seen to be much brighter than the interior. Reprinted with permission from [2]. DOI: 10.1103/PhysRev.124.1807 Copyright (2016) by the American Physical Society.

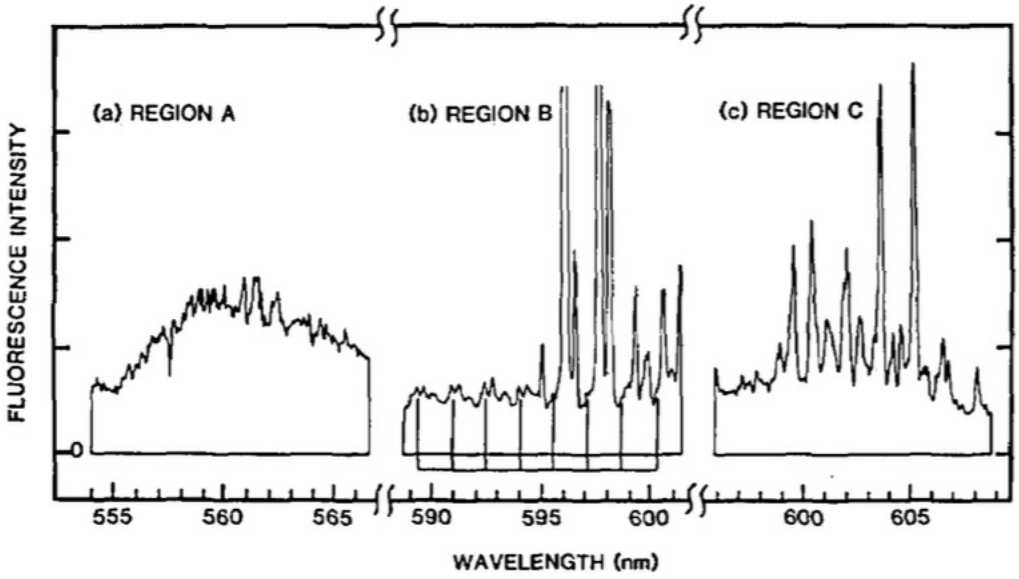

Figure 2: The first observation of a droplet laser, reprinted with permission from [13]. The three different regions correspond to (A) the peak in the fluorescence spectrum which overlaps with the tail of the absorption region, (B) has reduced absorption, but the fluorescence is starting to tail off, (C) has no absorption but a slightly lower fluorescence again. 595nm is the transition region where the gain exceeds the loss. The three different plots show the shift from no lasing to lasing. The strong peaks in (B) and (C) are the lasing modes.

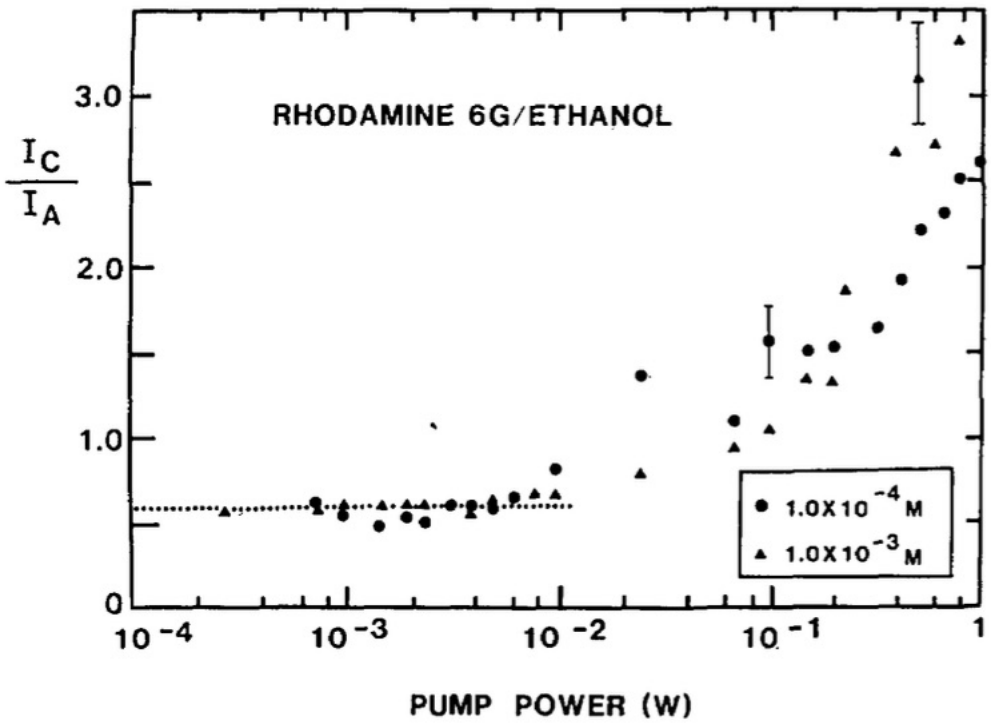

Figure 3: The threshold plot for the first droplet laser, reprinted with permission from [13]. This shows a characteristic threshold plot typical for all such droplet lasers, here for a Rh6G/ethanol droplet, and a threshold of $\sim 10^{-}2W$. I_C/I_A is the ratio of the intensity in region (C) to that in region (A) from figure 2

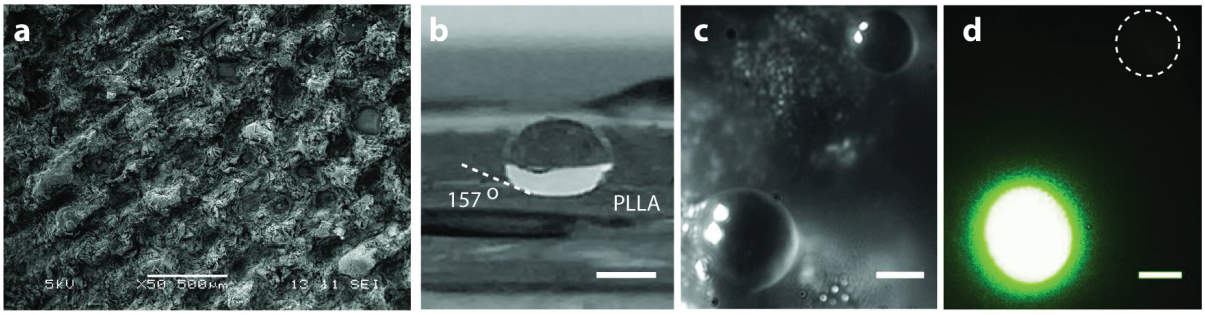

Figure 4: Droplets on a superhydrophobic surface. (a) An SEM image of a PLLA surface. (b) Droplet on a surface simialr to that in (a). (c) and (d) Brightfield and fluorescence image of a vitamin doped droplet. In (d) the droplet in the dotted circle is outside the pump region and does not emit. Scale bar in (b) is 1mm and in (c) and (d) $10\mu m$. Reproduced with permission from [116]. Copyright Wiley-VCH Verlag GmbH & Co. KGaA.

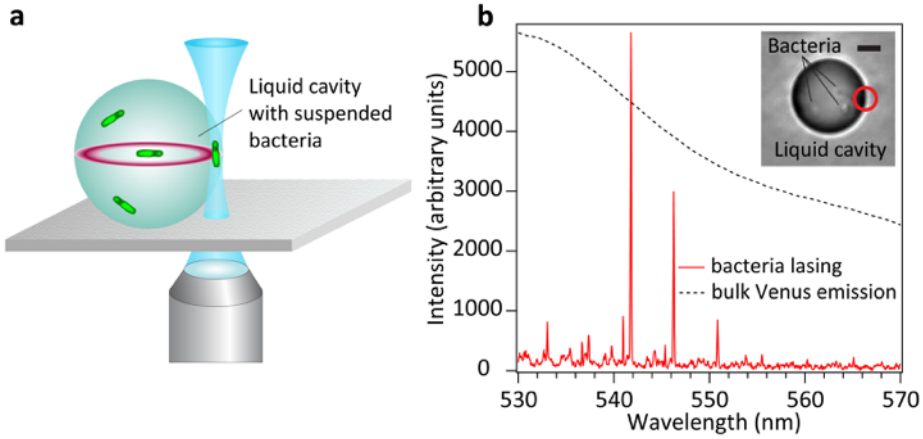

Figure 5: The bacterial laser. In (a) the droplet containing the bacteria sits on a superhydrophobic surface and is pumped at the edge form below. In (b) the output spectrum is shown, with the laser spectrum in the solid line, and the bulk emission of the Venus fluorescent protein in a dotted line. The inset shows an experimental image of a droplet containing the ~ 7 cells. The red circle is the point of laser excitation. Scale bar is $5\mu m$. Reproduced from [60] with permission from The Royal Society of Chemistry.

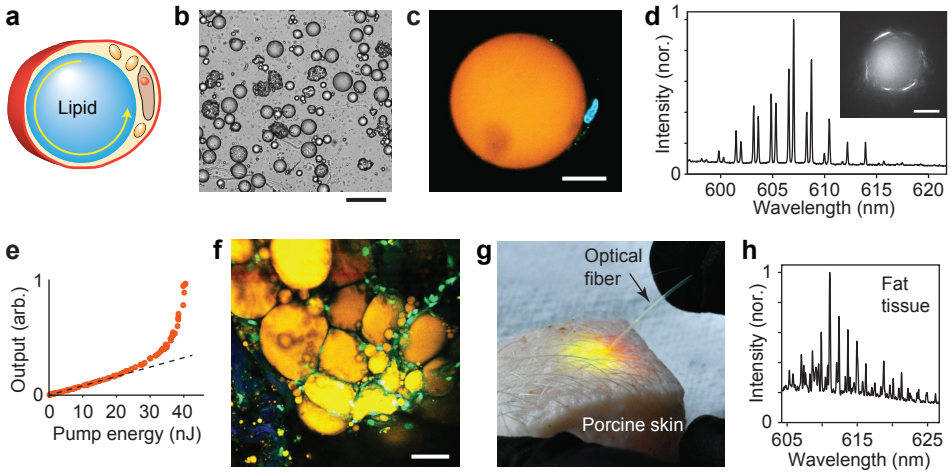

Figure 6: An overview of adipocyte droplet lasers. (a) Shows an adipocyte within a lipid droplet. (b) Experimental image of adipocytes. (c) Confocal image of an adipocyte showing a large lipid droplet (orange) which occupies the majority of the cell volume. The cell nucleus is in blue. (d) Lasing spectrum from a $45\mu m$ adipocyte; the inset shows a fluorescence image of the lasing droplet. (e) Output energy (in arb. units) against pump energy (nJ). The dashed line is the fit to the fluorescence output below the threshold point. (f) Two-photon confocal image of adipocytes in fat tissue. The yellow comes from injected Nile red dye. (g) An in-situ cellular laser. The optical fibre provides the pump light to the tissue after injection with Nile red dye and collagenase. (h) Output spectrum from the tissue in (g). Reprinted by permission from Macmillan Publishers Ltd: Nature Photonics [89], copyright (2015)

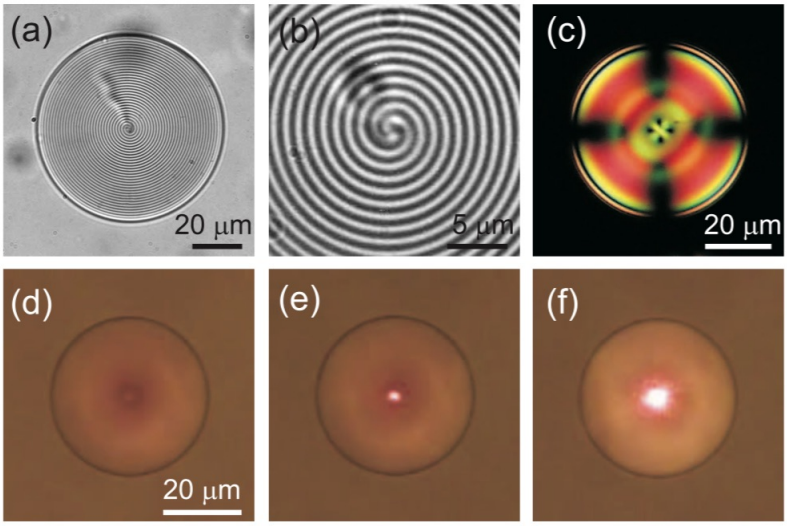

Figure 7: Liquid crystal laser droplets. (a) An experimental image of a liquid crystal droplet in glycerol with pitch of $2.2\mu m$. (b) Close up image of the droplet in (a). Viewed in the direction of parallel to the disclination line. (c) Liquid crystal droplet exhibiting a photonic bandgap, viewed under white light illumination using crossed polarisers. (d)-(f) Omnidirectional laser output: (d) below threshold, (e) at threshold, (f) well above threshold. Reproduced from [117] with permission.

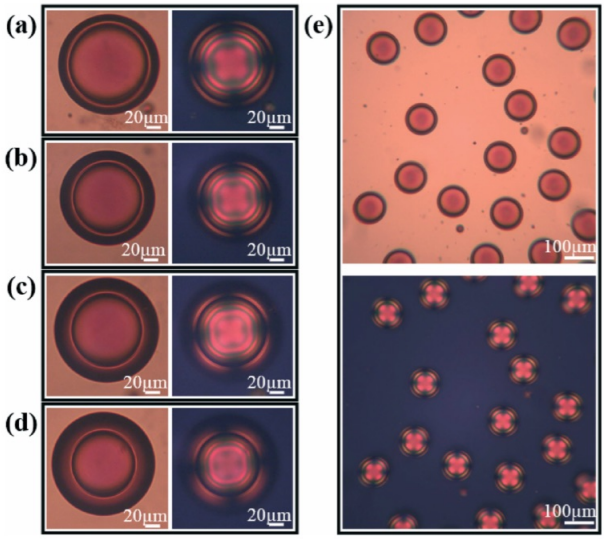

Figure 8: (a)-(d) show experimental images and polarised images (second column) of dye doped cholesteric liquid crystal droplets. The outer shell is $\sim 140 \mu m$. The shell thickness is $13 \mu m$ in (a), $17 \mu m$ in (b), $22 \mu m$ in (c) and $28 \mu m$ in (d). In (e) the monodispersity of the droplets is shown. Reproduced from [125] with permission from The Royal Society of Chemistry.

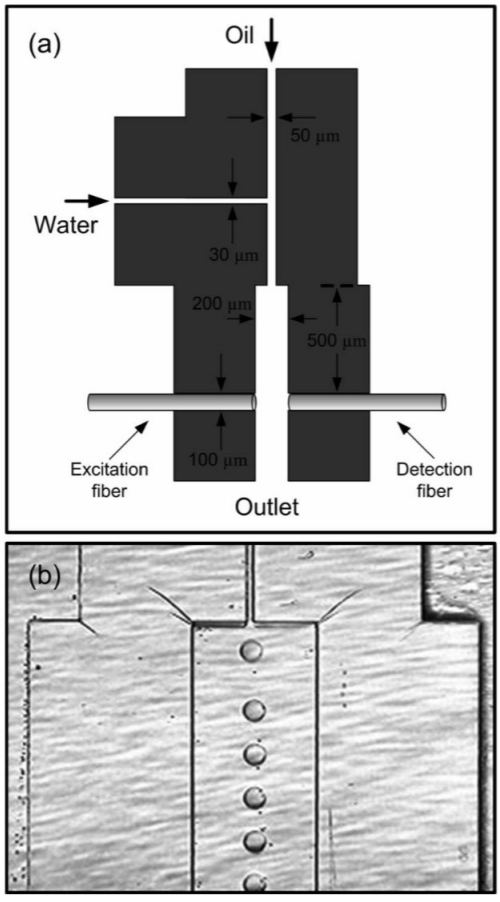

Figure 9: Microfluidic T-junction device capable of producing emulsion lasing droplets. (a) is a schematic of the device showing dimensions. (b) is an experimental image of the device in use to produce droplet. Reproduced from [134] with permission.

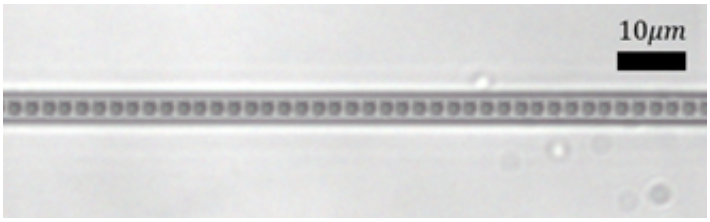

Figure 10: Image of an array of microdroplets in a microfluidic cavity capable of acting as a distributed feedback mirror. Reprinted from [143], with the permission of AIP Publishing.

(a) (b)

Figure 11: Droplets embedded within an elastomer matrix before and after deformation of the elastomer. Reproduced from [146] with permission.

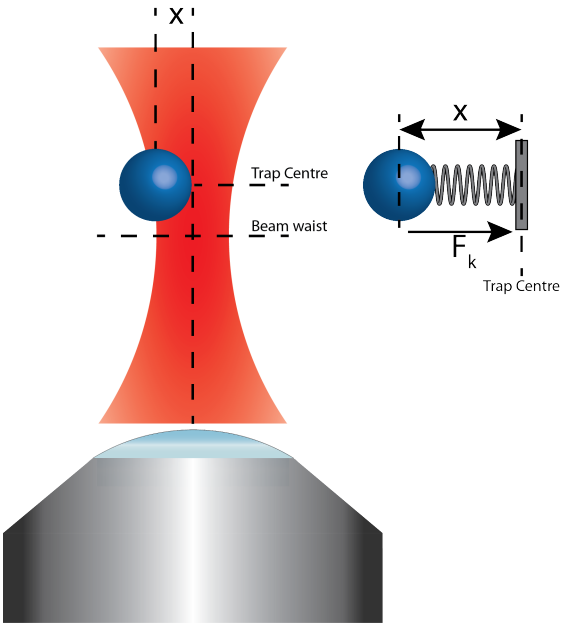

Figure 12: Optical tweezers attract particles to the most intense part of a highly focussed laser beam, in an analagous manner to a particle attached to a Hookean spring. A trapped particle will typically sit just above the beam waist, and the force on the particle is proportional to the displacement x from the optical axis. Figure courtesy of Dr Craig McDonald.

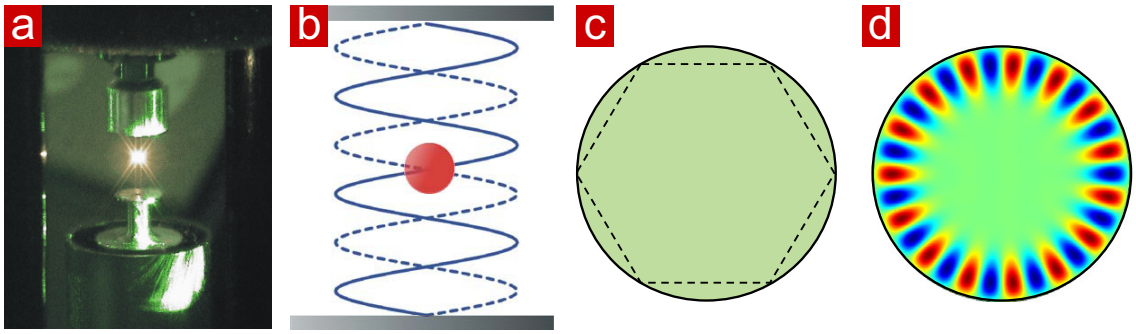

Figure 13: Acoustic levitation of laser droplets. (a) Shows an acoustic levitator device holding a lasing droplet. (b) The ultrasonic standing wave is able to trap a droplet in a pressure node. (c) WGM propagation in a spherical resonator. (d) Numerical simulation of a WGM mode in a 2D cavity. Reproduced from [164] with permission.

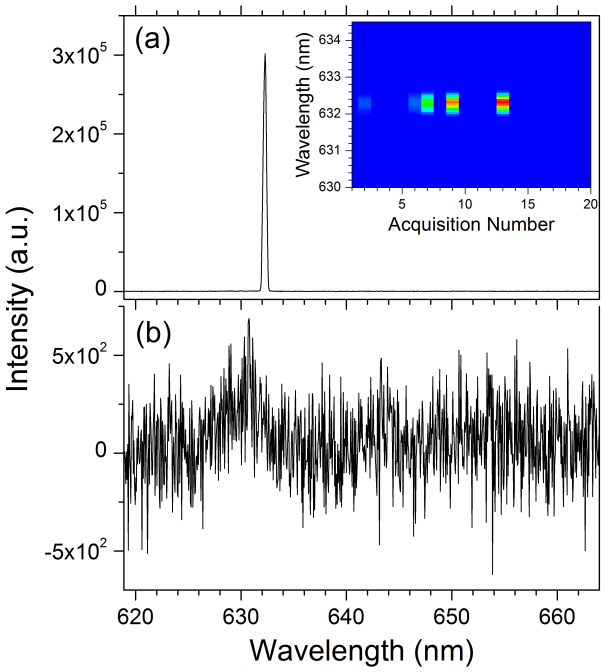

Figure 14: Raman lasing: (a) Spectrum from a 12.4nm diameter droplet exhibiting Raman lasing. (b) The spectrum from a droplet during the period where no-lasing occurs. The inset in (a) shows consecutive spectra illustrating this "on-off" behavior. Reproduced from [170] with permission.